



2018 Oral Presentations

PN 1. Time to Intervention Affecting Outcomes in Pediatric Nerve Injuries following Supracondylar Humerus Fractures

Megan E Friend, MD; Elizabeth A Newman, MD; Daniel Bracey, MD, PhD; Shea Comadoll, BS; Rebecca Senehi, BS; Zhongyu Li, MD, PhD

Wake Forest, Winston-Salem, NC

Introduction: Supracondylar humerus fractures are the most common pediatric elbow fractures, and nerve injury is a well-documented complication associated with these fractures. While most nerve injuries following supracondylar humerus fractures spontaneously resolve, other injuries require operative intervention by a nerve specialist. The aim of this study was to determine if time from injury to surgical intervention affects clinical outcomes in nerve injuries following pediatric supracondylar humerus fractures.

Materials and Methods: We performed a retrospective chart review of pediatric patients treated by the senior author for nerve injuries following supracondylar humerus fractures between 2006 and 2016. Sixteen patients with nerve injury requiring surgical intervention were identified. Chart review was performed to identify date of injury, fracture pattern, time to intervention by the senior author, and neurologic outcomes. British Medical Research Council scores for muscle strength and sensation were used to gauge recovery. A correlation analysis was performed to determine the effect on time to intervention on neurologic recovery.

Results: Average time to treatment by the senior author was 8.2 ± 5.5 mo. The majority of fractures in this group were Gartland type III supracondylar fractures (62.5%). The most commonly injured nerve was the ulnar (56%), followed by the median (31%), and radial (19%). Surgical indications included neuropathic pain, worsened neurologic exam after initial reduction, muscle atrophy, nerve conduction study findings, and lack of recovery at the time of referral. There was a statistically significant correlation of decreased time to surgery and improved outcomes when patients were treated <6 months from injury (Spearman correlation coefficient $r = -0.54$, $p = 0.04$).

Conclusion: Our study reveals that a decreased delay to surgery improves neurologic outcomes in pediatric patients with neurologic injury following supracondylar humerus fractures. Increased index of suspicion for more severe neurologic injury should be prompted by fractures with >100% displacement, presence of vascular compromise, open and ipsilateral fractures, neuropathic pain, and worsening neurologic exam following reduction. While a larger scale study is needed to further validate our findings, this study indicates the need for earlier referrals to a nerve specialist when there is neurologic compromise following a pediatric supracondylar humerus fracture, such that intervention can take place within 6 months of injury.

PN 2. Reverse End to Side Anterior Interosseous Nerve to Ulnar Nerve Transfer for Severe Ulnar Neuropathy

Christopher D Doherty, MD, MPH, FRCS(C)¹; Thomas Miller, MD, FRCPC¹, Sol Gregory, MD, FRCS(C)²; Brett Byers, MD, FRCS(C)¹; Douglas C. Ross, MD, MEd, FRCS(C)³

¹Western University, London, ON, Canada; ²Campbell River Hospital, Campbell River, BC, Canada; ³Roth | McFarlane Hand and Upper Limb Centre, Division of Plastic Surgery, University of Western Ontario, London, ON, Canada

Purpose

The purpose of this study is to evaluate the reverse end to side anterior interosseous nerve (AIN) to ulnar nerve transfer for various forms of severe ulnar neuropathy.

Methods

This study is a retrospective analysis with approval from Western University Biomedical Ethics review board. Chart review was performed for consecutive patients presenting to our institution between January 1st 2013 and January 31st 2016 who underwent AIN to ulnar nerve reverse end to side transfer for severe ulnar neuropathy (intrinsic muscle wasting and weakness). All procedures were performed by two plastic surgeons with a subspecialty practice in peripheral nerve surgery. Medical Research Council (MRC) intrinsic strength, DASH, and Patient Rated Ulnar Nerve Evaluation (PRUNE) survey scores were reviewed. A subset of patients is presented with formal strength testing. Electromyography was used to determine if reinnervation was evident at an earlier than expected time post-operatively.

Results

Forty-five patients were reviewed. The mean follow-up was 16 months. Nine patients underwent nerve transfer for closed trauma, six for laceration and 30 for severe compressive ulnar neuropathy at the elbow (McGowan grade 3). Mean post-operative MRC scores for first dorsal interossei was comparable and not statistically significant between all groups: 3.11, 3.0 and 3.02 respectively. All groups had statistically significant improvements in MRC grade from pre-operative values. Regarding intrinsic strength, 79% of patients achieved MRC grade 3 or greater, 58% grade 4 and 6% grade 5. The mean time (months) to presence of nascent units on EMG was 7.33, 6.92 and 6.6 respectively, which is earlier than expected. In a subset of patients, mean pinch strength (kg) was 7.67 kg in the affected hand versus 11.72 in the unaffected hand.

Conclusions

Reverse end to side nerve transfer appears to improve intrinsic strength and clinical outcomes for patients with various forms of severe ulnar neuropathy. Results are similar between groups thus demonstrating expanding indications for this nerve transfer.

PN 3. Electrophysiologic Outcomes of AIN End to Side Transfer for Severe Cubital Tunnel Syndrome; Preliminary results.

Matthew WT Curran, MD; Akiko Hachisuka, MD, PhD; Michael J Morhart, MD, MSc; Jaret L. Olson, MD; K. Ming Chan, MD
University of Alberta, Edmonton, AB, Canada

Introduction: Cubital tunnel syndrome is the second most common compression neuropathy. In severe cases, functional outcomes following surgical decompression of the cubital tunnel are poor. This in large part is due to the substantial distance between the site of injury and the target hand muscles. To circumvent that challenge, an end to side (ETS) nerve transfer to the ulnar nerve using a branch of the anterior interosseous nerve to the pronator quadratus muscle has gained increasing popularity. However, whether the donor motor axons are able to grow through the coaptation to the target muscles is unknown. The purpose of this study was to determine the relative contributions of the AIN and the ulnar nerve to the motor recovery.

Methods: In a prospective series of cubital tunnel patients with severe axonal loss, decompression of ulnar nerve at the cubital tunnel and an end to side transfer AIN to the deep motor branch of the ulnar nerve was completed. To evaluate the contributions of the AIN and the ulnar nerve to the hypothenar muscle, motor nerve conduction studies and motor unit number estimation (MUNE) were done before surgery and at 3, 6 and 12 months following surgery. The results were analyzed using non-parametric statistical techniques.

Results: Of the 10 patients enrolled, 7 had a minimum of 6 months follow-up with a median period of 8 {6-12 [median(IQR)]}. Patients were all male with a median age of 69 (57-74). There was no evidence of axonal growth from the AIN to the hypothenar muscles in any of the patients. MUNE at the last follow-up [11(6-111)] remained unchanged from baseline [12(7-22); $p=0.61$].

Conclusions: There is no electrophysiologic evidence of axons crossing from the AIN following an end to side transfer. All motor axons innervating the hypothenar muscles originate from the ulnar nerve.

PN 4. Magnetic Resonance Neurography of Traumatic And Non-traumatic Peripheral Trigeminal Neuropathies

John Randall Zuniga, DMD, MS, PhD; Igor Tikhonov, DDS, MD; Cyrus Mistry, DDS, MD; Riham Dessouky, MD; Avneesh Chhabra, MD

University of Texas, Dallas, TX

INTRODUCTION: Clinical neurosensory testing (NST) is currently the gold-standard for the diagnosis of traumatic and non-traumatic peripheral trigeminal neuropathies (PTN) but exhibits both false positive and negative results when compared to surgical findings and frequently delays treatment decisions as the results are dependent upon patients' subjective responses and observer skill. We tested the hypothesis that Magnetic Resonance Neurography (MRN) of PTN can serve as a diagnostic modality similar or better than NST by correlating NST, MRN and surgical findings.

MATERIALS & METHODS: Sixty patients from 4/2015 to 5/2017 with traumatic and non-traumatic PTN of varying etiologies and Sunderland classifications underwent NST followed by MRN at 1.5T and 3.0 T scanners. The protocol included 2D and 3D imaging, including diffusion imaging and isotropic 3D PSIF (0.9mm voxel). The MRN findings were read by two readers in consensus in the light of clinical findings, but blinded to the side of abnormality. The MRN results were summarized using Sunderland Classification. In 25 patients, surgery was performed and Sunderland Classification was assigned based on surgical photos and/or histology. Agreement between MRN and NST/Surgical classification was evaluated using Kappa statistics. Pearson's Correlation Coefficient (PCC) was used to assess the correlation between continuous measurements of MRN/NST and surgical classification.

RESULTS: Twenty males and 40 females, mean age 41, ranging 12 to 75, with 54 complaints of altered sensation of the lip/chin/or tongue, including 16 with neuropathic pain and 4 with no neurosensory complaint were included. Third molar surgery (n=29) represented the most common cause of traumatic PTN. MRN was indeterminate in none of the cases. Assuming one nerve abnormality per patient, the lower class was accepted, a Kappa of 0.57 was observed between MRN and NST classification. A Kappa of 0.5 existed between MRN and Surgical findings with a PCC of 0.67.

CONCLUSIONS: MRN anatomically maps PTN and stratifies the nerve injury and neuropathies with moderate to strong agreement with NST and surgical findings for clinical use. The application of a non-invasive objective modality like MRN to determine the classification and characteristics of an injured or abnormal trigeminal nerve earlier than NST can be tested in prospective studies in the future as it could serve as an important technique for outlining treatment decisions and determining patient outcomes.

PN 5. Nerve Transfer Versus Muscle Transfer to Restore Elbow Flexion After Pan Brachial Plexus Injury: A Cost-Effectiveness Analysis

Arvin Raj Wali, BA; David Rafael Santiago-Dieppa, MD; Justin M. Brown, MD; Ross Mandeville, MD

University of California, San Diego, La Jolla, CA

Objective:

Pan brachial plexus injury (PBPI), involving C5-T1, disproportionately affects young males causing lifelong disability and decreased quality of life. The restoration of elbow flexion remains a surgical priority for these patients. Within the first six months of injury, transfer of spinal accessory nerve (SAN) fascicles via sural nerve graft or intercostal nerve (ICN) fascicles to the musculocutaneous nerve can restore elbow flexion. Beyond one year, free functioning muscle transplant (FFMT) of the gracilis muscle can be used to restore elbow flexion. We present the first cost-effectiveness model to directly compare the different treatment strategies available to a patient with PBPI. This model assesses the quality of life impact, surgical costs, and the possible income recovered through restoration of elbow flexion.

Methods:

A Markov model was constructed to simulate a 25 year-old-male with PBPI without signs of recovery 4.5 months after injury. The management options available to the patient are SAN transfer, ICN transfer, delayed FFMT, or no treatment. Probabilities of surgical success rates, quality of life measurements, and disability were derived from published literature. Cost-effectiveness was defined using incremental cost-effectiveness ratios (ICERs) defined by the ratio between costs of a treatment strategy and the quality of adjusted life years (QALY) gained. A strategy was considered cost-effective if it yielded an ICER less than a willingness-to-pay of \$50,000/QALY gained. Probabilistic sensitivity analysis was performed to address parameter uncertainty.

Results:

The base case model demonstrated a lifetime QALY of 22.45 in the SAN group, 22.0 in the ICN group, 22.3 in the FFMT group and 21.3 in the no treatment group. The lifetime costs of income lost through disability and interventional/rehabilitation costs were \$683,400 in the SAN group, \$727,400 in the ICN group, \$704,900 in the FFMT group, and \$783,700 in the no treatment group. Each of the interventional modalities was able to dramatically improve quality of life and decrease lifelong costs. A Monte Carlo probabilistic sensitivity analysis demonstrated that at a willingness-to-pay of \$50,000/QALY gained, SAN transfer dominated in 88.5% of iterations,

FFMT dominated in 7.5% of iterations, ICN dominated in 3.5% of iterations, and no treatment dominated in 0.5% of iterations.

Conclusion: Our model demonstrates that nerve transfer surgery and muscle transplant are cost-effective strategies in the management of PBPI. These reconstructive neurosurgical modalities can improve quality of life and lifelong earnings through decreasing disability.

PN 6. Peripheral Nerve Transfers in the Treatment of Cervical Spondylolytic Amyotrophy

Douglas C Ross, MD MEd FRCS(C)¹; TA Miller, MD²; Charmaine Baxter, MD¹; Christopher Doherty, MD, FRCSC¹

¹Western University, London, ON, Canada; ²St. Joseph's Health Centre, University of Western Ontario, London, ON, Canada

Purpose: Cervical Spondylolytic Amyotrophy (CSA) is an uncommon disorder characterised by progressive, disabling upper extremity atrophy and weakness. Vascular insufficiency involving the anterior horn cell has been implicated. Cervical decompression approaches have produced variable results. The purpose of this paper is to report the use of nerve transfers to restore upper extremity function in CSA.

Methods: Eight patients with CSA were treated and reviewed. Pre-operative imaging and neurosurgical evaluation were completed in all. Comprehensive electrodiagnostic assessment to assess for peripheral nerve deficits as well as the status of potential donor nerves was undertaken. MRC strength testing pre- and post-operatively was completed. Patient-rated outcomes were assessed using a DASH questionnaire. Electromyographic findings at 5 and 12 months post-operatively were recorded.

Results: Seven patients demonstrated clinical, electrodiagnostic and imaging evidence of CSA at the C5/6 (proximal type) levels while one was of the “distal” type (C8/T1). All had been assessed in neurosurgical consultation and judged not to be candidates for decompressive surgery based upon criteria associated with poor outcomes (MRC grade <2, duration of symptoms, low CMAP amplitudes). All demonstrated marked wasting in the affected myotomes. Pre-operative electromyography demonstrated either single or no motor units in affected myotomes. Average age was 64.9 years with the majority being male (7 of 8). Mean duration of severe weakness pre-operatively was 13.2 months. The majority of patients were treated with “triple nerve transfers” to restore function of the suprascapular, axillary and musculocutaneous nerves. Average followup was 22.2 months (8-68). One patient died from metastatic bowel cancer 15 months post-operatively. Of patients with adequate post-operative followup, the average increase in elbow flexion was MRC 3+ (with restoration of absent supination), and the average increase in shoulder abduction was MRC 2+. EMG evidence of reinnervation was first observed at 5 months post-operatively and was used to trigger a course of rehabilitation emphasizing neuromuscular stimulation, biofeedback and neuroplasticity. Patient-rated DASH scores showed significant improvement.

Conclusions: CSA is an uncommon but highly disabling disorder. Nerve transfers should be considered for patients who are poor candidates for decompressive neurosurgical procedures.

Outcomes of nerve transfer surgery are encouraging despite advanced age and prolonged pre-operative weakness.

PN 7. The Effect of Fascicular Composition on Ulnar to Musculocutaneous Nerve Transfer (Oberlin Transfer) in Neonatal Brachial Plexus Palsy

Brandon W Smith; MD, MS; Nick Chulski, BA; Ann Little, MD; Kate Wan-Chu Chang, MA, MS; Lynda Yang, MD, PhD
University of Michigan, Ann Arbor, MI

Introduction: Neonatal brachial plexus palsy (NBPP) continues to be a problematic occurrence impacting approximately 1.5 per 1000 live births in the United States, with 10-40% of these infants experiencing permanent disability. These children lose elbow flexion, and one surgical option for recovering elbow flexion is the Oberlin Transfer. Published data supports the use of the ulnar nerve fascicle that innervates the flexor carpi ulnaris as the donor nerve in adults, however, no analogous published data exists in infants. This study investigated the association of ulnar nerve fascicle choice with functional elbow flexion outcome in NBPP.

Methods: Our study included a retrospective cohort of 13 infants who underwent ulnar to musculocutaneous nerve transfer for NBPP at a single institution. We collected patient demographics, clinical characteristics, active range of motion (AROM), and intraoperative nerve monitoring (IOM) data (using 4 ulnar nerve index muscles). Standard statistical analysis compared pre- and post-operative motor function improvement between specific fascicle transfer (1-2 muscles for either wrist flexion or hand intrinsics) and non-specific fascicle transfer (>2 muscles for wrist flexion and hand intrinsics) groups. The institutional review board (IRB) approved the study.

Results: The average age at initial clinic visit was 2.9 months old, and the average at surgical intervention was 7.4 months. All NBPP were unilateral; the majority were female (61%), Caucasian (69%) with right-sided NBPP (61%), and Narakas III-IV (54%). IOM recordings for the fascicular dissection revealed a donor fascicle with non-specific innervation in 6 (46%) subjects, the remaining 7 (54%) patients had donor fascicles with IOM recordings specific innervation. At 6-month follow-up, the AROM improvement in elbow flexion in adduction was 38° in specific fascicle transfer versus 36° in non-specific fascicle transfer with no statistically difference (P=0.93). The AROM improvement in supination was 66° in specific fascicle transfer versus 84° in non-specific fascicle transfer with no statistically significant difference (P=0.72).

Discussion: Our results demonstrate that both specific and non-specific fascicle transfers lead to functional recovery, but that the composition of the donor fascicle had no impact on early outcomes. In infants, ulnar nerve fascicular dissection places the ulnar nerve at risk for iatrogenic damage. Our data suggests that the use of any motor fascicle, specific or non-specific, produces

similar results and that the Oberlin transfer can be performed with less intrafascicular dissection, less time of surgical exposure, and less potential for donor site morbidity.

PN 8. Thoracic Outlet Syndrome Decompression in Adolescents

Heather L Minton, BS¹; Erin E Ransom, MD¹; Bradley L Young, MD²; Martim C Pinto, MD¹; Brent A Ponce, MD¹; Richard D Meyer, MD¹

¹University of Alabama at Birmingham, Birmingham, AL; ²Carolinas Medical Center, Charlotte, NC

Introduction: Neurogenic Thoracic Outlet Syndrome (NTOS) is relatively uncommon in the general population and less common in adolescents. This study aims to characterize surgical outcomes following NTOS decompression in adolescents and identify relationships between perioperative factors and surgical outcomes.

Methods: A retrospective review was conducted of adolescent patients surgically treated for NTOS at a single institution from 2000 to 2015. Perioperative factors and functional outcomes were assessed using the quick Disabilities of Arm, Shoulder, and Hand (quick-DASH) survey, Cervical-Brachial Symptom Questionnaire (CBSQ), the 10-point visual analog scale (VAS) for pain, and the Single Assessment Numeric Evaluation (SANE). Study data were collected and managed using REDCap electronic data capture tools. Analysis of variance was conducted using Statistical Analysis Software and Microsoft Excel.

Results: Study population consisted of 63 adolescents aged 8-21 at time of presentation, with a median age of 15 years. The dominant arm was affected in 65% of patients. Mechanisms of injury primarily involved overuse (28; 47.5%) or trauma (13; 22.1%). Surgical intervention was selected in patients whom conservative management was unsuccessful. The surgical procedure was tailored to each patient and commonly involved neurolysis of the brachial plexus (98.4%), anterior scalenectomy (93.8%), middle scalenectomy (87.5%), and excision of anomalous soft tissue (40.6%). The average length of stay was 1.04 +/- 0.19 days. Repeat surgeries (2, 3.1%) were rare. Cervical ribs or other osseous anomalies were seen in 14.1% of patients, while soft tissue anomalies were seen in 73.4% of patients. Long term follow-up averaging 64.2 months identified an improvement in the VAS of 6.14 points from a preoperative average score of 8.0 and postoperative average score of 2.14. The average SANE score before surgery was 26.9 and after was 85.24. The average postoperative quickDASH and CBSQ scores were 12.23 with a range from 0 to 52.27 on a 100-point scale and 27.62 with a range from 0 to 92 on a 120-point scale, respectively.

Conclusion: Following failure of non-operative treatment, surgical decompression relieves symptoms and allows reliable return to recreational activities in adolescent patients with NTOS.

PN 9. New Open and Arthroscopic-assisted Approaches of the Axillary Nerve

Andrés A. Maldonado, MD, PhD^{1,2}; Bassen T Elhassan, MD²; Allen Bishop, MD²; Alex Shin, MD²; Robert J Spinner, MD²

¹*BG Unfallklinik, Frankfurt, Germany*, ²*Mayo Clinic, Rochester, MN*

Introduction: Previous studies have described a segment of the axillary nerve (AN) that cannot be surgically explored through standard open surgical approaches (blind zone). The aim of this study is to evaluate the feasibility of combining the standard posterior approach to the AN with the use of the arthroscope to visualize all segments of the AN; and determine the AN length that can be seen through standard and extended anterior, axillary and posterior approaches.

Material and methods: Ten fresh frozen shoulders in five adult human torsos were included in the study. A standard posterior approach was performed on four shoulders and dry arthroscopy was performed through the surgical opening in an attempt to visualize all segments of the AN. A surgical clip was applied to the most proximal and anterior segments of the AN that could be visualized with the arthroscope. A standard open deltopectoral approach was then performed to determine the exact location of the surgical clip and its relation to the origin of the AN. Then, we attempted to explore the AN through 3 different surgical approaches (each approach was performed in 2 shoulders): a standard and extended anterior, axillary and posterior approaches. Surgical clips were used to mark the AN length that was visualized through each approach.

Results: Using the arthroscopic-assisted approach, all segments of the AN (including the blind zone) were visualized from the quadrilateral space to their origin from the posterior cord in all four specimens. The surgical clip was found at an average 1 cm (range from 0.5 to 1.5 cm) from the origin of the AN from the posterior cord. Compared to the standard approaches, the extended anterior, axillary and posterior approaches improved the visualization of the AN by 3.6 cm, 1.5 cm and 2.8 cm respectively.

Conclusions: This cadaveric study shows that it is feasible to visualize all segments of the AN (including the blind zone) using this novel arthroscopic-assisted approach that combines the use of the standard posterior approach to the AN with dry arthroscopic exploration. Clinical studies are necessary to evaluate the utility of this novel approach. None of these extended approaches independently was sufficient to expose the entire course of the AN.

PN 10. Quantitative Electromyography as a Predictor of Nerve Transfer Outcome

Ross Mandeville, MD; Justin M. Brown, MD

University of California, San Diego, La Jolla, CA

Introduction: The pre-operative assessment for nerve transfer surgery is key to a successful outcome, however reliance on clinical exam with only basic neurophysiological studies is the norm. Significantly more neurophysiological information can be obtained pre-operatively to aid in planning of nerve transfer surgery - in particular, quantitatively electromyography (qEMG). Usual neurophysiological evaluation lacks granularity, often only grading a muscle as mild, moderate, or severe. Within the severe grade, greater precision can be obtained through quantifying the number of motor units (MU) within the interference pattern. This study evaluates the ability of pre-operative donor nerve qEMG using MU counts to predict the post-operative force outcome in nerve transfer surgery.

Methods: We performed a retrospective review of pre-operative donor nerve quantitative neurophysiology and post-operative recipient muscle force after at least one year follow-up. The quantitative technique applied was Motor Unit (MU) count, which was correlated with hand-held manometry, standardized as a percent of the contralateral arm, using multivariable linear regression with backward selection.

Results: Twenty-eight nerve transfer cases were included. The correlation between the donor nerve MU count and the recipient muscle strength was strong and highly significant (Fig. 1: $r = 0.67$, $p < 0.001$). Importantly, in these 28 cases, pre-operative Medical Research Council (MRC) grading did not predict strength outcome ($p > 0.54$).

Conclusions: The technique of qEMG Motor Unit count is a good predictor of strength outcome after nerve transfer surgery and could be considered useful in the evaluation and planning of patients undergoing nerve transfer surgery to aid in donor nerve selection. Caution is advised when relying solely on MRC grading to select donor nerves.

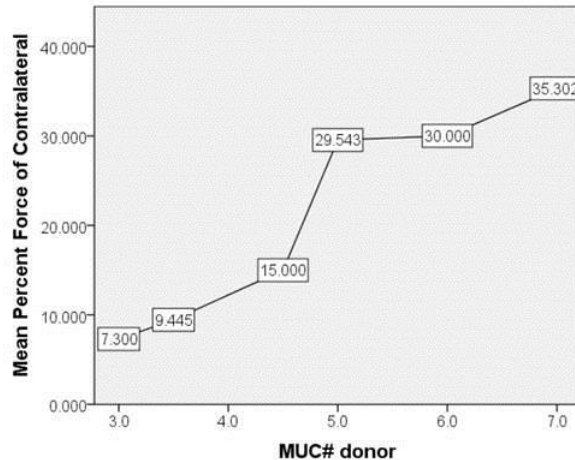


Figure 1. Graph depicting the relationship between *Motor Unit count* (MUC) and the *Force* outcome as a percent of the contralateral unaffected limb. MUC of 7 indicates at least 7 motor units ($r = 0.67$, $p < 0.001$).

PN 11. Motor Functional Recovery after Median Nerve Reconstructions using Processed Nerve Allografts

Bauback Safa, MD¹; Timothy R Niacaris, MD, PhD²; Steven Maschke, MD³; John V Ingari, MD⁴; Jaimie T Shores, MD⁴; Harry Hoyen, MD⁵; Mickey Cho, MD⁶; Leon J Nesti, MD, PhD⁷; Gregory Buncke, MD¹

¹The Buncke Clinic, San Francisco, CA; ²UNT Health Science Center, Fort Worth, TX;

³Cleveland Clinic, Cleveland, OH; ⁴Johns Hopkins Medicine, Baltimore, MD; ⁵MetroHealth System, Cleveland, OH; ⁶San Antonio Military Medical Center, San Antonio, TX; ⁷Walter Reed National Military Medical Center, Bethesda, MD

Introduction Processed Nerve allografts (PNA) have seen increased utility for reconstruction of peripheral nerve injury. The RANGER® registry is an ongoing study that collects data on the utilization and outcomes of PNA (Avance® Nerve Graft, AxoGen) in peripheral nerve repair. Favorable outcomes have been demonstrated in an interim analysis of the expanding dataset. While a large proportion includes sensory nerve injuries due to the higher rates of incidence, the database also contains a significant number of major peripheral nerves repairs allowing for the evaluation of specific injury types. This current analysis was conducted to evaluate the motor functional outcomes after median nerve injuries repaired with PNA.

Materials & Methods The RANGER database was queried for median nerve transections repaired with PNA that met following criteria: nerve transections distal to the elbow, repairs within six months (180 days) after injury; a minimum of six months of follow-up assessments; documented relevant motor function assessments sufficient for outcome evaluation using the Medical Research Council (MRC) scale. For median nerve repairs at forearm level, motor function assessment included flexion of the thumb, index and middle fingers as well as the ability to form a composite fist; for repairs at wrist and recurrent motor branch level, assessment included palmar abduction of the thumb, flexion of the index and middle fingers at metacarpophalangeal joints. Meaningful recovery was defined as MRC scale \geq M3.

Results There were 18 median nerve repairs that met the inclusion criteria. Eight occurred at the forearm, eight at the wrist, and two at the recurrent motor branch level. Subjects in this cohort had a mean age of 41 ± 19 years. The average gap length of nerve injuries was 35 ± 21 mm. Subjects were followed for an average of 473 ± 168 days. Fifteen (83%) of the repairs reported a MRC scale of $\geq M3$. While complex injuries had longer gaps, no significant difference in meaningful recovery was seen between the groups. See Table 1. These results compare favorably to the rate of meaningful recovery with nerve autograft reported in the literature.

Conclusions Repair of median nerves using processed nerve allografts after injury resulted in promising motor functional recovery. Processed nerve allograft represents a viable option for reconstruction of mixed nerves injuries. Outcomes compared favorably to that of nerve autograft reported in literature.

Table 1: Result Summary			
	All	Laceration	Complex*
Number of repairs	18	11	7
Age (years) §	41 ± 19	46 ± 21	34 ± 14
Gap length (mm) §	35 ± 21	26 ± 9	49 ± 27
Pre-operative interval (days) ¶	6 (0, 133)	1 (0, 70)	14 (0, 133)
Follow-up (days) §	473 ± 168	482 ± 174	460 ± 156
Meaningful recovery (n)	15	9	6
Rate of meaningful recovery	83%	82%	86%

§ Age, gap length, follow-up days are presented as Mean \pm SD.
 ¶ Pre-operative interval is presented as Median (minimum, maximum)
 *Complex injuries include gunshot/blast, crush injury and surgical resection

PN 12. Regenerative Agonist-Antagonist Myoneural Interface for Neural Prosthetic Control

Shriya S Srinivasan, BS^{1,2}; Matthew J. Carty, MD³; Peter Calvaresi, BS¹; Anthony Zorzos, PhD¹; Tyler Clites, BS¹; Hugh Herr, PhD¹

¹*Massachusetts Institute of Technology, Cambridge, MA*, ²*Harvard Medical School, Boston, MA*,
³*Division of Plastic Surgery, Brigham and Women's Hospital, Boston, MA*

Introduction: During a standard amputation, nerves are transected, causing painful neuromas and rendering efferent recordings infeasible for robust prosthetic control. Furthermore, physiological agonist-antagonist muscle relationships are severed, precluding the generation of musculotendinous proprioceptive afferent signals. This afferent feedback is critical for joint stability, trajectory planning, and fine motor control. Here, we created and evaluated an Agonist-antagonist Myoneural Interface (AMI), a novel surgical paradigm for peripheral nerve interfacing, which reinstates the antagonist-agonist architecture native to intact musculoskeletal anatomy and provides a robust method for efferent and afferent signaling with motor nerves.

Materials & Methods: Tendons from two deinnervated, devascularized muscle grafts were surgically coapted to form an agonist-antagonist pair and secured to fascia in 7 murine subjects. Each graft was neurotized with either the peroneal or tibial nerve. After 4 months, we electrically stimulated the regenerated motor nerve of the agonist muscle while measuring the strains in each muscle, agonist EMG and the afferent ENG signal generated by the antagonist muscle. To isolate the dependence of afferent feedback on an agonist-antagonist structure, the linked muscles were separated. ENG and EMG signals from both muscles were measured in response to electrical stimulation. Finally, we performed histology of the harvested AMI to assess healing and regeneration.

Results: Monthly insertional EMG testing revealed reinnervation levels comparable to healthy muscles at 3-4 months after surgery. EMG from the agonist muscle proportionally scaled with stimulation amplitude (average $r^2 = 0.85$ for $n=7$) and yielded a proportional stretch in the antagonist muscle (range of strain: 0.08 ± 0.03 to 0.23 ± 0.14), but no co-contraction or EMG spikes. Furthermore, afferent signals were generated from the antagonist muscle and linearly correlated to the strains generated ($r^2 = 0.96$) (Fig 1 A, B). Once the agonist-antagonist link was severed, no afferent signals were generated (Fig 1C). Histology indicated regenerating myocytes, healthy neural tissue and viable muscle spindle fibers, primarily responsible for generating afferent signals in response to stretch.

Conclusions: In this study, validation of the AMI model resulted in graded efferent EMG and afferent ENG signals generated from functionally regenerated myoneural constructs. The AMI framework has the potential to enable robust peripheral nerve interfacing capable of natural efferent and afferent signaling in human subjects.

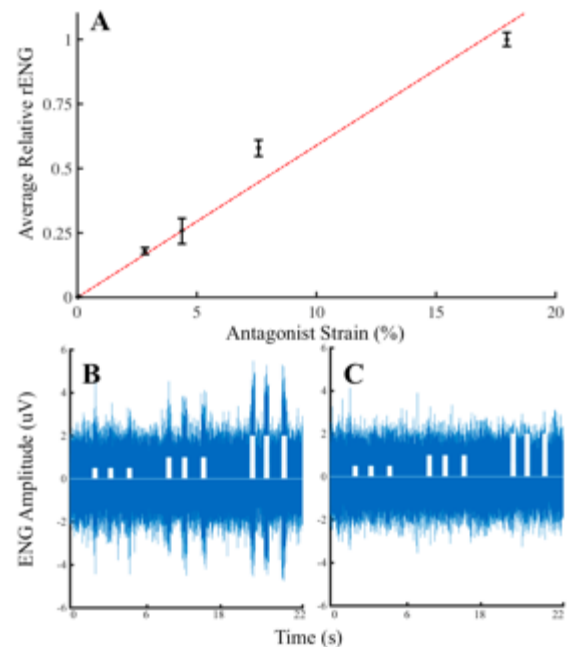


Fig 1. (Stimulation pulses (white) = 0.5, 1, 2 mA)

PN 13. Body-Worn Sensor Technology Captures Patient-Initiated Spontaneous Arm Movement after Reconstructive Surgery for Brachial Plexus Injury

Susan H Brown, PhD; Tanu Bhargava, MS; Serena J Saake, BS; Denise Justice, OTRL; Lynnette Rasmussen, OTRL; Kate Wan-Chu Chang, MA, MS; Samuel J Hertz, BS; Kevin C. Chung, MD, MS; Lynda Yang, MD, PhD

University of Michigan, Ann Arbor, MI

Introduction: Clinical assessment of function following reconstructive surgery for brachial plexus injury typically includes physician-elicited range of motion, muscle strength and self-reported disability. However, to what extent these measures predict patient-initiated arm movement following nerve reconstruction surgery is unclear. Recent advances in body-worn sensor technology provide a means of monitoring actual arm use in naturalistic settings following surgical reconstruction in this population. **Methods:** Clinical assessments of arm function (active range of motion (AROM), strength (MRC scale), and the Disabilities of the Arm, Shoulder, and Hand (DASH) questionnaire were completed on 10 patients (> 1 yr post-surgery, mean age: 43 y) who underwent either nerve transfer ($n=7$) or free functioning muscle transfer (FFMT, $n=3$) for brachial plexus injury. Patients then wore accelerometers (GT9X ActiGraph) on each wrist during waking hours for 7 consecutive days. The accelerometers measured arm motion in three planes and data were analyzed using ActiLife 6.13. **Results:** Compliance was excellent with an average weekly wear time of 110 hours. No adverse effects related to wearing the devices were reported. The mean ratio of arm use magnitude in the nerve transfer patients was .62 indicating that the amount of affected arm movement was 62% of the unaffected arm. In contrast, arm magnitude ratio was only .27 in the FFMT group. In the nerve

transfer group, affected arm use was correlated with both biceps strength ($r=0.79$) and elbow AROM ($r=0.81$). A very strong correlation was observed between arm use and DASH scores was observed ($r=0.93$). No correlations were seen in the FFMT group. Conclusions: We demonstrate that body worn sensor technology is a feasible approach to monitoring “real world” arm use in patients following surgery for brachial plexus injury. We suggest that our results support the continued use of nerve reconstruction for brachial plexus injury in the appropriate patients. In contrast, our preliminary results do not support the use of free muscle transfers for patients with total brachial plexus injury, but further research involving a larger patient sample is warranted.

PN 14. First Carpometacarpal Joint Denervation for Primary Osteoarthritis: technique and outcomes

Daniel P. Donato, MD; James Willcockson, MD; Leah Frazer, PA-C; Mark A. Mahan, MD
University of Utah, Salt Lake City, UT

Introduction: Pain at the thumb carpometacarpal (CMC) joint is one of the most common complaints in patients with osteoarthritis. The innervation of the first CMC joint is believed to arise from branches of the four principle nerves that surround it: the superficial branch of the radial nerve, palmar cutaneous branch of the median nerve, recurrent branch of the median nerve, and the lateral antebrachial cutaneous nerve. Using 2 small incisions, all the articular branches are able to be severed effectively relieving joint pain. There are small case series in Europe showing success of this procedure as the primary treatment modality, but the available studies are relatively small, and there are no published studies from North America. We sought to show efficacy of the procedure and increase the available body of literature for this procedure.

Material and Methods: We reviewed all patients who underwent first carpometacarpal (CMC) joint denervation at our institution between January 1, 2015 and May 1, 2017. These patients were prospectively assessed with preoperative pain scores and grip strength measurements using a Jamar Dynamometer. Patients were offered the surgery if they 1) had a positive response in grip strength after diagnostic injection; 2) had no evidence of CMC joint instability on exam. All patients underwent the same CMC denervation procedure through incisions at the volar wrist crease and dorsal first web space.

Results: A total of 9 patients and 11 first CMC joints underwent this operation. Prior to surgery, all patients reported poor function and significant levels of pain, with an average VAS of 7.1. All patients demonstrated improved grip strength at diagnostic injection. Post-operative VAS decreased to an average of 3.1 out of 10. All but one patient reported improvement in pain, and no patient reporting worsened pain. Grip strength increased from 36.9 foot/pounds preoperatively to 50.1 foot/pounds post-operatively. 8 of 9 patients reported satisfaction with the procedure and 1 was unsure. Complications were relatively low. One patient developed a post-operative wound infection requiring antibiotics, one develop a C6 radiculopathy, and on patient had persistent focal pain at the dorsal CMC joint, likely secondary to a missed dorsal branched during the denervation.

Conclusion: Thumb CMC denervation provides good pain relief and improvement in grip patients with osteoarthritis. This provides a good alternative for patients unable or unwilling to undergo more invasive procedures.

PN 15. High Sensitivity of EDX In Neonatal Brachial Plexus Palsy (NBPP) Warrants Increased Use In Pre-Operative Planning Of Nerve Reconstruction Strategies

Mary Catherine Spires, MD; Kate Wan-Chu Chang, MA, MS; Lynda Yang, MD, PhD
University of Michigan, Ann Arbor, MI

Introduction: Use of electrodiagnostic testing (EDX) for surgical decision-making in NBPP (incidence of 1-4/1000 live births) is controversial. Despite high inter-rater reliability for assessing the NBPP lesions (pre- vs post-ganglionic), EDX is routinely used less than imaging - and consequently less for planning the strategy for nerve reconstruction. Therefore, the purposes of this study are (1) to determine the sensitivity of EDX and (2) to compare the sensitivity of EDX with that of imaging in NBPP. Methods: We conducted a retrospective review of infants with NBPP from 2007 to 2017 at a single institution. Infants who underwent both pre-operative EDX and imaging (CT-myelogram, MRI) were included in the study. The findings of pre-operative EDX and imaging were compared to the surgical findings (gold standard) regarding NBPP nerve root pre-ganglionic and post-ganglionic lesions. Sensitivities of EDX vs. imaging were reported to evaluate performance accuracy of each pre-operative diagnostic tool. Results: Fifty-four infants (mean age of 6.9 months) were included in the study; the majority were female (57%), Caucasian (63%), and Narakas II-IV (72%). EDX demonstrated significant higher overall sensitivity for detecting post-ganglionic lesion at all nerve root levels: at C7, EDX demonstrated 92% sensitivity vs. imaging (73%, $P=0.006$); at C8, EDX was 88% sensitive vs. imaging (29%, $P=0.008$); at C5, EDX was 88% sensitive compared to imaging (84%, $P=0.7$); similarly, at C6, EDX was 97% sensitive vs. imaging (85%, $p=0.23$). For pre-ganglionic lesion that are detectable on imaging by the presence of pseudomeningoceles, the sensitivity of imaging at C5 was only

43% (compared to EDX at 14%, $P=0.7$). Likewise, C6 was similarly disappointing with sensitivity of 57% (compared to EDX at 39%, $P=0.23$). Imaging had expected higher sensitivities than EDX at C7 (EDX: 30% vs. imaging: 83%, $P=0.006$) and C8 (EDX: 38% vs. imaging: 67%, $P=0.008$) levels. Conclusions: We demonstrate that EDX has an overall high sensitivity in demonstrating post-ganglionic lesions in NBPP, and therefore, EDX is essential for pre-operative planning of nerve reconstruction strategies. Because EDX was poorly reputed as a surgical planning tool due to its reported poor ability to prognosticate, no prior study had addressed the sensitivity of EDX in determining the location/severity of individual nerve root lesions. We suggest that these results warrant the increased use of EDX in strategizing surgery.

PN 16. Predictors of Severity and Recovery in Virus-mediated Acute Flaccid Myelitis
Erin L Weber, MD, PhD; Mitchel Seruya, MD
University of Southern California, Los Angeles, CA

Background: Acute flaccid myelitis (AFM) is the sudden onset of limb paralysis following a viral illness. With eradication of the poliovirus, cases of AFM are extremely rare. However, clustered outbreaks of AFM in the United States and throughout the developed world are increasing, raising concern that another polio-like epidemic could be imminent. The purpose of this study was to identify predictors of disease severity and upper limb recovery in our regional population.

Methods: A retrospective chart review was performed to identify all cases of viral-related acute flaccid myelitis treated at our pediatric institution between 2014 and 2017. Patient age, sex, prodromal symptoms, time from viral illness to onset of paralysis, past medical history, and medical therapy (steroids, intravenous immunoglobulins, and fluoxetine) were reviewed. Functional deficits and improvements over time were assessed using the Medical Research Council (MRC) scale for muscle strength. Successful recovery for each muscle group was defined as \geq M3 function.

Results: Eight patients qualified for inclusion, with an age range of 2-13 years and an equal gender distribution. 75% had bilateral upper extremity paralysis. There was no correlation between disease severity and age, sex, prodromal symptoms, or time to onset of paralysis. In cases of bilateral paralysis, the degree and pattern of functional loss was not similar between limbs. All patients were managed with steroid, intravenous immunoglobulins, and/or fluoxetine therapy. Varied degrees of recovery were observed in 63% by the 6-month mark, with no correlation with the type of medical therapy (Table 1). Proximal upper extremity function, particularly shoulder abduction, was more frequently affected and

less likely to recover. The frequency of successful functional recovery was not related to the severity of initial paralysis. Interestingly, a history of asthma was common to those patients who showed no signs of recovery. Ultimately, nerve transfer procedures were recommended in 88% of patients to maximize function.

Conclusions: In acute flaccid myelitis, there are few clear predictors of disease severity, progression, and recovery. However, a history of asthma may predict more severe paralysis and decreased spontaneous recovery. If functional recovery is not evident by 6 months, long-term improvement is unlikely and surgical intervention is prudent. Nerve transfer should prioritize the shoulder and elbow, as these functions are most frequently and most severely affected.

Table 1. Functional recovery over time.
Values of 0-2 reflect persistent weakness, 3-5 reflect successful recovery

		Right upper extremity												Nerve transfer recommended
		Initial onset				6 months								
Patient age (yrs)	Patient sex	Shoulder abduction	Elbow flex / ext	Wrist flex / ext	Finger flex / ext	Shoulder abduction	Elbow flex / ext	Wrist flex / ext	Finger flex / ext	Shoulder abduction	Elbow flex / ext	Wrist flex / ext	Finger flex / ext	
1.8	F	0	0	0	0	0	0	0	0	0	0	0	0	Y
1.9	M	0	0	0	0	1	0	0	0	2	0	2	2	Y
2.7	F	1	0	0	-	4	4	1	4	4	4	4	4	Y
2.8	M	3	3	3	3	3	3	3	3	3	3	3	3	
3	F	3	3	3	3	3	3	3	3	3	3	3	3	
3.1	M	0	3	3	3	3	3	4	4	4	4	4	4	
6.8	F	0	0	0	0	3	2	0	0	2	3	4	1	Y
12.6	F	0	0	0	0	0	0	0	0	0	0	0	0	Y

		Left upper extremity												Nerve transfer recommended
		Initial onset				6 months								
Patient age (yrs)	Patient sex	Shoulder abduction	Elbow flex / ext	Wrist flex / ext	Finger flex / ext	Shoulder abduction	Elbow flex / ext	Wrist flex / ext	Finger flex / ext	Shoulder abduction	Elbow flex / ext	Wrist flex / ext	Finger flex / ext	
1.8	F	4	4	4	4	4	4	4	4	4	4	4	4	
1.9	M	2	2	2	2	2	2	2	2	2	2	2	2	Y
2.7	F	2	2	-	-	4	4	2	4	2	3	2	4	Y
2.8	M	0	0	0	-	2	4	0	1	4	4	5	4	Y
3	F	0	0	0	0	0	0	4	4	4	4	4	4	
3.1	M	0	0	0	0	1	0	0	0	0	4	0	0	Y
6.8	F	0	3	1	4	4	4	0	4	3	5	5	5	Y
12.6	F	1	1	1	1	1	1	4	4	3	4	4	4	

PN 17. Treatment and survival in malignant peripheral nerve sheath tumors: a SEER database analysis per tumor site

Enrico Martin, BS^{1,2}; Ivo S. Muskens, BS^{1,2}; Timothy R. Smith, MD, PhD, MPH¹; Marike L.D. Broekman, MD, PhD, JD^{1,2}

¹Brigham & Women's Hospital, Harvard Medical School, Boston, MA; ²University Medical Center Utrecht, Utrecht, Netherlands

Background: Currently, literature is lacking data on differences across tumor sites in survival and treatment in malignant peripheral nerve sheath tumors (MPNSTs). The Surveillance, Epidemiology, and End Results (SEER) database provides a means of assessing possible predictive factors of survival and treatment strategies.

Methods: MPNST cases were obtained from the SEER program from 1973-2013. Tumor sites were recoded into: intracranial, spinal, head and neck (H&N), limbs, core, and unknown. Patient and tumor characteristics, treatment modalities, and survival were extracted. Overall survival was assessed using univariate and multivariate cox-regression hazard models and Kaplan-Meier survival curves were constructed per tumor site for overall survival (OS) and disease specific survival (DSS). Only primary tumors were used for survival analyses.

Results: 3267 MPNST patients were registered in SEER; 167 intracranial (5.1%), 119 spinal (3.6%), 449 H&N (13.7%), 1022 limb (31.3%), 1307 core (40.0%), and 203 unknown (6.2%). The largest tumors were found in core (size: 80.0mm, IQR: 60.0-115.0mm) and limb sites (size: 70.0mm, IQR: 40.0-100.0mm), and the smallest were intracranial (size: 37.4mm, IQR: 17.3-43.5).

Intracranial tumors were resected least frequently (58.1%), whereas spinal tumors were most often resected (83.0%). Gross total resection was most commonly achieved in spinal tumors (42.6%) and least frequently in core tumors (24.9%). Radiation was administered in 35.5% intracranial and 41.8% limb MPNSTs. Independent factors negatively influencing survival were: older age, male sex, black race, no surgery, not gross total resection, large tumor size, high tumor grade, H&N site, and core site (all $p < 0.05$). Intracranial and pediatric tumors showed superior survival (both $p < 0.05$). Patients with intracranial tumors showed superior OS (**Figure 1**) and DSS curves (**Figure 2**), whereas core tumors had the worst OS and DSS ($p < 0.001$).

Conclusion: Treatment modalities, extent of resection, and tumor size vary across primary tumor sites. Best survival was seen in intracranial MPNSTs, whereas core and H&N tumors had a worse prognosis.

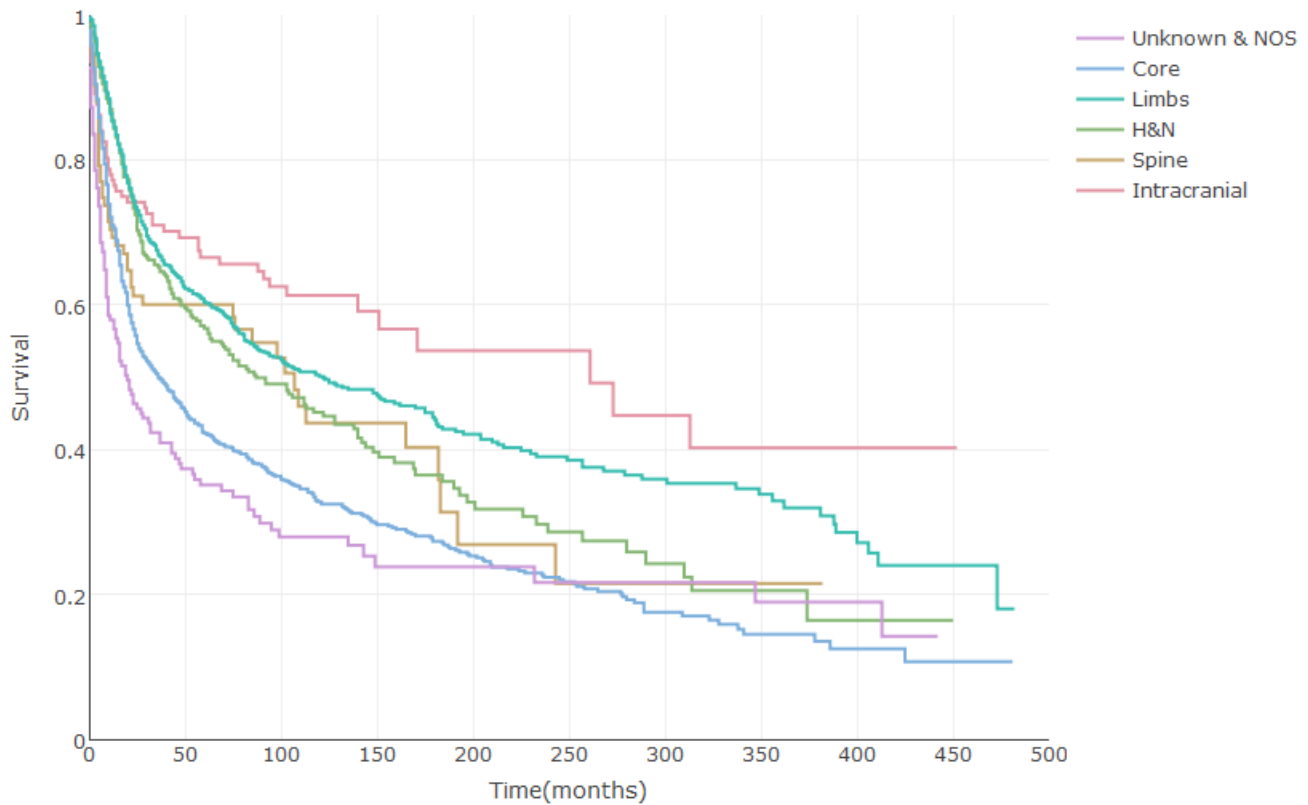
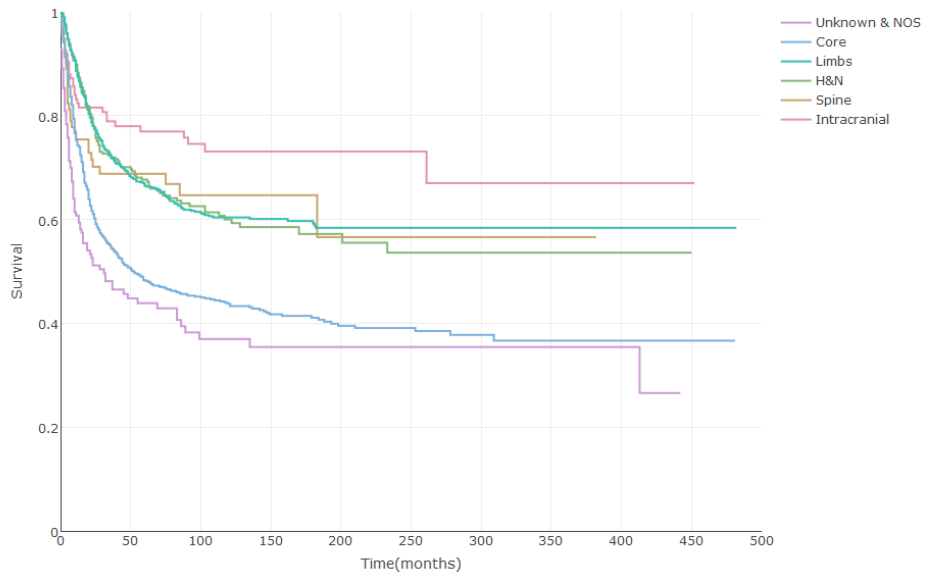


Figure 1. Overall Survival in MPNST per Site

Figure 2. Disease-Specific Survival in MPNST per Site



PN 18. A Proximal Crush Nerve Injury Prevents Neuropathic Pain

Ian Wood, BS; Jane Wang, BS; Lauren Schellhardt, BS; Matthew Wood, PhD; Amy M Moore, MD

Washington University School of Medicine, Saint Louis, MO

Introduction: Neuropathic pain after nerve injury is not well understood, and current surgical treatment modalities for pain demonstrate variable success. The purpose of our study was to investigate the therapeutic effects of a proximal nerve crush on pain behavior following sciatic nerve transection injury.

Methods: Rats (n=16) were randomly assigned to experimental and sham therapy groups and received a sciatic nerve transection proximal to the trifurcation and the distal nerve was transposed. Nociception was evaluated by application of acetone to the mid-plantar surface of the hindpaw of both injured and uninjured limbs every two days for the first week and then weekly thereafter. Total time spent flinching (lifting or licking of the ventral surface) was recorded. At 2 weeks following transection, one experimental group received a crush injury 5-10 mm proximal to the site of transection, and the control group received a sham therapy. Behavior testing was continued following these therapies as before until 5 months post-therapy.

Results: Cold allodynia testing indicated that sciatic nerve transection resulted in elevated nociceptive pain behavior in the afflicted limb. A crush injury proximal to the site of transection two weeks after injury prevented development of cold allodynia hypersensitivity as compared to sham controls. This response was sustained for the duration of the experiment (five months).

Conclusions: These findings suggest that a proximal crush injury may be used therapeutically to prevent neuropathic pain following nerve injury, and could potentially provide an adjunctive strategy of treatment and/or prevention of painful neuromas.

PN 19. Neuroma Prevention with Prophylactic Regenerative Peripheral Nerve Interface Placement

Carrie A Kubiak, MD; Paul S. Cederna, MD; Stephen WP Kemp, PhD; Theodore A Kung, MD
University of Michigan, Ann Arbor, MI

Introduction: Regenerative Peripheral Nerve Interfaces (RPNI) can be used to treat symptomatic end neuromas that develop after major limb amputation. Symptomatic neuromas occur in approximately 30-40% of individuals after limb loss and phantom limb pain affects 70-95% of these patients. We investigate the potential of prophylactic RPNI to prevent neuroma formation and to mitigate the experience of phantom limb pain. Furthermore, we examine the potential complications resulting from the addition of prophylactic RPNI to major limb amputation surgery.

Materials & Methods: At the time of amputation, RPNI were performed by implanting transected peripheral nerves into free muscle grafts harvested from the amputated limb. Patients who underwent major limb amputation with simultaneous prophylactic RPNI implantation were identified. A retrospective chart review was performed to ascertain patient demographics, indication for amputation, level of amputation, characteristics of postamputation pain, perioperative pain management strategies, and postoperative complications. During follow up, all patients were evaluated for symptomatic neuromas and phantom limb pain through detailed history and physical exam.

Results: RPNI were prophylactically implanted in 38 patients who underwent 44 major limb amputations. The mean patient age was 46 years (range 3-79) and mean follow up was 301 days (range 6-897). The most common indication for amputation was osteomyelitis from chronic wounds (n=11, 25%) followed by trauma (n=8, 18%). Below knee amputations comprised the majority of subjects (n=34, 77%). Major postoperative complications were defined as events that resulted in admission or surgery; one patient (2.6%) suffered residual limb infection necessitating operative washout. Minor complications included delayed wound healing (16%) and surgical site infection managed on an outpatient basis (9%). Fourteen patients (37%) reported symptoms of phantom limb pain during their postoperative course. Zero of the 142 surgical sites (0%) demonstrated any clinical evidence of symptomatic neuroma postoperatively.

Conclusions: Prophylactic RPNI in major limb amputees resulted in a considerably lower incidence of both symptomatic neuromas and phantom limb pain as compared to published rates in the literature. Implantation of prophylactic RPNI did not contribute to increased morbidity compared to standard amputation techniques. These findings suggest that prevention of peripheral nerve pain following major limb amputation may diminish the central pain mechanisms that lead to phantom limb pain. This pilot study supports prospective investigation of using RPNI to significantly reduce postamputation pain.

PN 20. Novel Experimental Surgical Strategy to Prevent Traumatic Neuroma Formation by Combining a 3D-printed Y-tube with an Autograft

Anne Bolleboom, BSc¹; Godard C.W. de Ruiter, MD²; J Henk Coert, MD; PhD³; Bastiaan Tuk, BS¹; Joan C. Holstege, PhD¹; Johan W. van Neck, PhD¹

¹*Erasmus University Medical Center, Rotterdam, Netherlands;* ²*Neurosurgery, Medical Center Haaglanden, The Hague, Netherlands;* ³*University Medical center Utrecht, Utrecht, Netherlands*

Object. Traumatic neuromas may develop following nerve injury at the proximal nerve stump, which can lead to neuropathic pain. These neuromas are often therapy resistant and excision of the neuroma frequently leads to recurrence. In this study we present a novel surgical strategy to prevent neuroma formation based on the principle of the centro-central anastomosis (CCA), but instead of directly connecting the nerve ends to an autograft a loop was created using a three-dimensional (3D) printed polyethylene Y-shaped conduit with an autograft in the distal outlets.

Methods. The 3D printed Y-tube with autograft was investigated in the rat sciatic nerve transection model in which the Y-tube was placed on the proximal sciatic nerve stump and a peroneal graft was placed between the distal outlets of the Y-tube to form a closed loop. This model was compared to a centro-central anastomosis model, in which a loop was created between the proximal tibial and peroneal nerve with a peroneal autograft. Additional control groups consisted of the closed Y-tube and the extended arm Y-tube. Results were analyzed after 12 weeks survival with nerve morphometry for the occurrence of neuroma formation and axonal regeneration in plastic semi-thin sections.

Results. Among the different surgical groups, the Y-tube with interposed autograft was the only model that did not result in neuroma formation after 12 weeks survival. In addition, a 13% reduction in the number of myelinated axons regenerating through the interposed autograft was observed in the Y-tube with autograft model. In the centro-central anastomosis model we also observed a decrease of 17% in the number of myelinated axons, but in this model neuroma formation was still present. The closed Y-tube resulted in minimal nerve regeneration inside the tube together with extensive neuroma formation before the entrance of the tube. The extended arm Y-tube model clearly showed that the majority of the regenerating axons merged into the Y-tube arm, which was connected to the autograft, leaving the extended plastic arm almost empty.

Conclusions. This pilot study shows that our novel 3D printed Y-tube model with interposed autograft prevents neuroma formation, making this a promising surgical tool for the management of traumatic neuromas.

PN 21. Surgical Management of Post-Traumatic Supraorbital and Supratrochlear Neuromas

Robin S Yang, MD; Chopra Karan, MD; Eric Howard Williams, MD; A. Lee Dellon, M.D., PhD
The Johns Hopkins University School of Medicine, Baltimore, MD

Introduction Trauma to the supraorbital ridge is an under-appreciated and underdiagnosed source of pain. Blunt and penetrating trauma, aesthetic surgery, and craniofacial/neurosurgical procedures are potential sources of injury to the supraorbital (SO) and or supratrochlear (ST) nerves. Pain related to injuries of these nerves can cause intractable headaches, and dysesthesias in the frontal-orbital facial region. Management of these nerve injuries is relatively under-reported. We present our experience with surgical management of SO and ST neuromas with nerve resection and implantation of the proximal nerve deep within the orbital cavity.

Methods and Materials A retrospective, chart-review, study was performed. Patients included into the study were those who had direct trauma/injury to the supra-orbital region. All patients included in the study had failed at least one year of medical management and pain control prior to surgery. All patients had symptom relief with a pre-surgical nerve block of the SO and ST nerves. All patients included received similar surgical intervention, which was to divide the SO and ST nerves within the orbit through an upper blepharoplasty incision. 15 patients were identified who met the inclusion criteria. The patients age ranged from 18-75 with an average of 50.5 years. Mechanism of Injury: Trauma = 12 Craniofacial/Neurosurgery = 2 Cosmetic procedure = 1. Unilateral Resection = 7 Bilateral Resection = 5

Results Mean follow up: 16 month. Pre-operative VAS: 9.4/10 Post-Operative VAS: 2.6/10 ($p < .001$). All patients had a good or excellent outcome. No pain with extraocular eye movement. No wound complications.

Conclusion This is the first report of successful treatment of neuromas of the SO and ST nerves by resection of neuroma and placement of the proximal ends within the orbital cavity. There was satisfactory relief of neuropathic pain with this surgical technique without any pain within the implantation site with ocular movement.

Figures:

A.

B.



A. SO Nerve prior to resection B. SO Nerve resection prior to

implantation

PN 22. Real-Time Visual Assessments of Nerve Damage: Second Harmonic Generation Microscopy as a Novel Imaging Modality

Matthew J Gluck, BS; Christina M Beck, PhD; Todd A Rubin, MD; Paul J Cagle, MD; Michael R Hausman, MD

Mount Sinai Hospital, New York, NY

Introduction: Orthopaedic injuries of the extremities are often complicated by confounding peripheral nerve trauma. Damaged nerves that appear macroscopically intact or exhibit an incomplete EMG disturbance pose the biggest clinical dilemma. This leaves care providers unable to predict the degree to which an injured nerve will recover, potentially delaying necessary surgical intervention. Second Harmonic Generation Microscopy (SHG) may provide a novel, reliable, real-time assessment of epineurial collagen damage, allowing surgeons to accurately predict the degree of axonal damage present in peripheral nerves. In this study, we demonstrate the utility of SHG microscopy to detect nerve damage *in vivo*.

Materials and Methods: Right and left median nerves of 16 Sprague-Dawley rats (n=16) were carefully exposed using micro-surgical techniques. Using a custom made stretch applicator right median nerves were stretched to 20% corresponding to a high strain injury (HS) and held for 5 minutes, while left median nerves (SC) served as a sham control, only being placed in the applicator for 5 minutes with no stretch applied. Subjects were then placed directly on a microscope stage and imaged using a multi-photon laser scanning microscope with a 25x/1.05 numerical aperture water immersion multi-photon lens. All rats were imaged at day 0 (immediately after injury), at which point half were sacrificed for conventional histology, and half were imaged again at 1 week following the injury, before being sacrificed for conventional histology.

Results: Immediately after injury (day 0), SHG images of SC median nerves exhibited parallel collagen fibers with linear, organized alignment. HS nerves demonstrated artifacts indicative of nerve damage consisting of wavy, undulating fibers, with crossing fibers and tears, as well as a decrease in linear organization. At 1 week post injury, SC nerves demonstrated the same organization at later time points, while HS nerves exhibited increasing structural changes including increased fiber gapping, suggesting the presence of Wallerian degeneration as correlated to an increase in digestion chambers visible in histological sections.

Conclusion: SHG microscopy may offer the ability to detect not only an acute neural stretch injury, but also assess the longitudinal structural changes associated with Wallerian degeneration. SHG microscopy has demonstrated its utility as a tool for surgeons to predict the probability of spontaneous recovery, and thus allow for earlier intervention.

PN 23. A Dual Nerve and Muscle Injury is Partial Recovered with Brain-Derived Neurotrophic Factor Stem Cell treatment

Brian Michael Balog, BS^{1,2,3}; Xiaoyi Yuan, MD⁴; Dan Li Lin, MD⁵; Mei Kuang, PhD¹; Brett Hanzlicek, MS⁶; Hao Yan, MD⁷; Margot Damaser, PhD⁸

¹Cleveland Clinic Lerner Research Institute, Cleveland, OH; ²Louis Stokes Veteran Service Hospital, Cleveland, OH; ³University of Akron, Akron, OH; ⁴Tongji Hospital Huazhong University of Science and Technology, Hankou, Wuhan, China; ⁵Louis Stokes Veteran Affairs Medical Center, Cleveland, OH; ⁶Louis Stokes Veterans Affairs Medical Center, Cleveland, OH; ⁷Xuanwu Hospital Capital Medical University, Beijing Shi, China; ⁸Louis Stokes Veteran Affairs Hospital, Cleveland, OH

Stress urinary incontinence (SUI) is highly correlated with childbirth when the pudendal nerve and the muscle it innervates, the external urethral sphincter, are both injured, creating a dual muscle & nerve injury. While neuroregeneration is promoted by brain-derived neurotrophic factor (BDNF), BDNF inhibits myogenesis. Mesenchymal stem cell (MSC) secretions contain BDNF and accelerate recovery in a SUI rat model. We hypothesize that BDNF is the active factor in accelerated recovery via MSC secretions.

An anti-BDNF shRNA lentivirus vector was used to create BDNF Knockdown (KD) rat bone marrow-derived MSCs. A scrambled sequence (scrambled) served as a transfection control. Media was sorted and concentrated 50x to produce concentrated conditioned media (CCM) containing the secretions of MSCs. Media that was not conditioned by the cells served as concentrated control media (CM). Rats underwent either sham injury (SI) or pudendal nerve crush (PNC) & vaginal distension (VD) as a model of SUI. CCM or CM (300 μ l) was injected intraperitoneally 1 hour and 1 week after the injury. SI rats received CM; PNC+VD rats received CM, CCM, KD CCM or scrambled CCM. Leak point pressure (LPP) and pudendal nerve sensory branch potential (PNSBP) were recorded three weeks after injury. The urethra and pudendal nerve were harvested for anatomic assessment. ANOVA followed by a Student-Newman-Keuls posthoc test was used to determine statistically significant differences between groups ($p < 0.05$).

LPP was not significantly decreased in scrambled (36.0 \pm 3.1 cm H₂O) or CCM (51.1 \pm 3.1 cm H₂O) groups compared to SI (40.9 \pm 3.3 cm H₂O), but was significantly decreased in PNC+VD + CM (28.3 \pm 2.1 cm H₂O) and KD CCM (31.1 \pm 2.5 cm H₂O) groups. CM treatment of PNC+VD (399 \pm 100 Hz) was the only group with a significant decrease in PNSBP firing rate compared to SI (977 \pm 93 Hz). KD CCM, scrambled CCM, and CCM treated PNC+VD groups showed healthier neuromuscular junctions in the external urethral sphincter compared to PNC+VD+CM. However, pudendal nerve axons were less dense with PNC+VD treated with KD CCM than other treatment groups.

Reducing BDNF in CCM reduces neuroregeneration of the pudendal nerve and LPP after PNC+VD, but does not reduce pudendal nerve firing rate or neuromuscular junction recovery, suggesting that complete recovery is likely slowed with reduced BDNF. BDNF is most likely not the only factor important for recovery from the dual nerve and muscle injury of childbirth that results in SUI.

PN 24. Surgical Interventions for the Treatment of Painful Neuroma: A Comparative Meta-Analysis

Louis H Poppler, MD, MSCI; Rajiv P Parikh, MD, MPHS; Miles Bichanich, BS; Kelsey A Rebehn, MD; Carrie Bettlach, FNP; Susan E. Mackinnon, MD; Amy M. Moore, MD
Washington University School of Medicine, St. Louis, MO

Purpose: No consensus on the optimal treatment of painful neuromas exists. Our objective was to synthesize all available data on outcomes following surgical management of painful neuromas and to examine the role of surgical technique and confounding on outcomes.

Methods: In accordance with the PRISMA guidelines, we performed a literature search of Embase, Scopus, PubMed, Cochrane library, and ClinicalTrials.gov. Studies measuring the efficacy of the surgical treatment of painful neuromas in the extremities were included in this meta-analysis (excluding Morton's neuroma and compression neuropathies). Surgical treatments were categorized as excision only, excision and transposition, excision and cap, excision and repair, or neurolysis and coverage. Data on the proportion of patients with a meaningful reduction in pain was collected and a random effects meta-analysis was performed. The effects of confounding, study quality, and publication bias were examined with stratified, meta-regression, and bias analysis.

Results: 54 articles met inclusion criteria, many with multiple treatment groups (Figure 1). Outcomes reporting varied significantly and few studies controlled for confounding. Overall, surgical treatment of neuroma pain was effective in 77% patients [95% confidence interval (CI): 73-81] No significant differences were seen between surgical techniques (Figure 2). In stratified analysis, "excision and transposition" and "neurolysis and coverage" were significantly more likely to result in a meaningful reduction in pain for patients with neuroma pain for greater than 24 months prior to their operation and in patients who had one or more prior operations ($p < 0.05$) (Figure 3-4).

Conclusions: Surgical treatment of neuroma pain is helpful when patients are carefully diagnosed and managed. Standardization of surgical techniques, outcomes, and confounding reporting are needed in future studies to elucidate patient and surgical factors that predict successful outcomes and aid with patient selection.

PN 25. Algorithm for 3-Tesla MR Neurography-guided Nerve Blocks to distinguish Sitting Pain Origin from either Pudendal Nerve or Posterior Femoral Cutaneous Nerve

Lena Sonnow, MD; A. Lee Dellon, M.D., PhD; Jan Fritz, MD

The Johns Hopkins University School of Medicine, Baltimore, MD

Introduction:

Inability to sit is a significant disability. A neural origin for this disability can be from either the pudendal nerve (PN) or the posterior femoral cutaneous nerve (PFCN). While surgical approaches to resect or perform neurolysis of these injured nerves have been described, the diagnostic approach to identify the source of the pain has not. It is the purpose of this report to describe the algorithm we have been using successfully for the past two years.

Materials and Methods:

A total of 20 patients who had pain with sitting and no history of injury to the coccyx were included. Each patient had undergone 3-Tesla MR neurography of the pelvis that was negative for nerve entrapment and neuroma formation. The differential diagnostic block of the PN and the PFCN were performed under 3-Tesla MR neurography guidance. For each block, 3 ml of 0.5% ropivacaine were used. PN blocks were performed in the Canal of Alcock. PFCN blocks were performed in the subgluteal space near the ischial tuberosity. After each block, the area of numbness and relief of pain with sitting were noted. Pain relief of 50% or more was considered a positive pain response. Based on the results of the nerve blocks, either the PN or PFCN or both were operated upon. For the PN, either the sacrotuberous ligament was divided if there were rectal symptoms, or the perineal branch of the pudendal nerve was resected if there were no rectal symptoms. The PFCN was resected and proximally implanted into the gluteus muscle. Successful surgery was defined as pain relief of at least 50% and ability to sit again.

Results:

Of the 20 patients, 18 had a positive response to either PN, PFCN, or both blocks, whereas 2/20 (10%) patients had a negative response to either block. The differential nerve block identified the PN as the source of pain in 8/20 (44%), PFCN in 8/20 (44%), and both in 2/20 (12%). Based upon the surgical outcome, the differential blocks had a sensitivity of 90% (95% confidence interval, 68-99%), positive predictive value of 90% (68-99%), and accuracy of 83% for diagnosing the pain generating nerve and predicting pain relief after surgery.

Conclusions:

An algorithm is presented for the diagnosis of sitting pain of neural origin that has a sensitivity and positive predictive value of 90% in managing this difficult clinical problem.

PN 26. Studies on Wnt Genes in Neuroma-in-Continuity and During Nerve Regeneration

Arie C Van Vliet, MSc¹; Martijn Tannemaat, MD, PhD²; Martijn JA Malessy, MD, PhD³; Fred De Winter, PhD¹; Joost Verhaagen, PhD¹

¹*Netherlands Institute for Neuroscience, Amsterdam, Netherlands*, ²*University of Leiden, Leiden, Netherlands*, ³*Department of Neurosurgery, Leiden University Medical Center, Leiden, Netherlands*

Introduction. A neuroma-in-continuity (NIC), formed following a human nerve lesion, impedes functional recovery. The mechanisms that underlie the formation of a NIC are poorly understood. Wnt ligand genes encode highly conserved glycoproteins with roles in development and tissue repair. Here we investigated Wnts and their receptors in NIC and in the injured rat sciatic nerve.

Materials and Methods. Wnt gene expression was investigated by microarray and qPCR. The biological activity of selected Wnt ligands was studied in embryonic and adult rodent dorsal root ganglion (DRG)-based repulsion and neurite outgrowth assays. Functional interference in a rat nerve injury and repair model was performed with lentiviral vectors encoding Wnt-inhibiting-factor 1 (WIF1) or in transgenic mice with Schwann cell specific mutation of Wnt5a.

Results. The expression of multiple genes of the Wnt family, including Wnt5a, are upregulated in NIC tissue. In the injured rat sciatic nerve, four Wnt-gene clusters with temporal expression profiles corresponding to specific phases of the regeneration process were identified. Schwann cells in the NIC and in the injured nerve are the source of Wnt5a, whereas the Wnt5a receptor Ryk is expressed by axons in the NIC. Wnt5a, Wnt5b and Wnt4 were chosen for functional studies because they are induced in the NIC formed following injury to a human nerve (Wnt5a) and in the injured rat nerve (Wnt5a, Wnt5b and Wnt4). Wnt5a, -5b and -4 promote neurite outgrowth of embryonic DRGs. Cultured naïve adult DRGs neurons did not significantly respond to Wnt5a, but displayed a clear trend towards enhanced neurite growth, whereas conditioned DRG neurons are inhibited by Wnt5a. This switch in responsiveness may be due to changes in Wnt-receptor composition. Indeed, DRG neurons without Ryk (obtained from Ryk^{0/0} mice), exhibit dramatically enhanced outgrowth in response to Wnt5a compared to wildtype DRGs, whereas overexpression of specific Wnt receptors (or combinations) either stimulates or impedes neurite growth in a DRG-like cellular screen. Collectively, these data suggest that the receptor composition affects the neurite outgrowth response of sensory neurites to Wnt ligands. Preliminary in vivo studies showed that functional perturbation of multiple ligands with the Wnt sequestering protein WIF1 or genetic deletion of a single Wnt gene (Wnt5a) in Schwann cells slows down axon regeneration.

Conclusion. Wnt signalling has a role in the regeneration process of an injured nerve. Increasing our understanding of these and other signalling pathways in the injured nerve is of importance to the development of nerve repair strategies.

PN 27. Novel Use of Peripheral Nerve Stimulation in the Treatment of Pain/Shoulder Subluxation Resulting from Stroke Hemiplegia

Rashad Albeiruty, MD; Ted Edward Claflin, MD; Lynda Yang, MD, PhD; Kate Wan-Chu Chang, MA, MS; Srinivas Chiravuri, MD
University of Michigan, Ann Arbor, MI

Introduction: Pain and shoulder subluxation resulting from stroke hemiplegia can be refractory to medical pain management. Theoretically, axillary nerve stimulation can activate the deltoid and teres minor shoulder muscles, thereby reducing pain and shoulder subluxation. As opposed to the general application of peripheral nerve (PN) stimulation to address painful sensory peripheral neuropathies, we aim to demonstrate the novel utility of PN motor stimulation to ameliorate symptomatic sequelae of central nervous system conditions such as stroke. **Methods:** Two hemiplegic patients with pain and shoulder subluxation underwent placement of a minimally-invasive neuromodulation system (PN stimulator comprising an implanted lead, external pulse transmitter (EPT), and conductive electrode, that are controlled by a small, hand-held patient programming device) after failing maximal conventional rehabilitation methods. The following pre- and post-operative measurements were used: numeric pain scale to assess shoulder pain and finger breadth to assess shoulder subluxation. Additionally, active range of motion (AROM) for shoulder flexion/extension, abduction/adduction, and internal/external rotation, along with muscle power (MRC grade) for the aforementioned movements were recorded. **Results:** Both patients had significant reductions in their numerical pain scores post-operatively: 7/10 to 0/10 for the first patient and 6/10 to 0/10 for the second patient. Subluxation as measured by finger breadth decreased from 1 to 0 for both patients. Motor strength for all arm muscle groups improved from 0/5 to 4/5 for the first patient and from 3/5 to 4/5 for the second patient. For the first patient, AROM improved from 0° for all arm movements to 45° abduction/45° flexion/10° extension/10° external rotation/5° internal rotation. For the second patient, AROM improved from 0° to 90° abduction/90° flexion/10° extension/10° external rotation/5° internal rotation. **Conclusions:** We demonstrate that axillary nerve stimulation significantly reduced pain, shoulder subluxation, motor strength, and AROM in patient experiencing hemiplegic shoulder pain after stroke. The innovative addition of neuromodulation to conventional rehabilitation and medical treatments may be superior to conventional treatment alone for managing hemiplegic shoulder pain refractory to conservative treatments. Additionally, these results indicate that neuromodulation may represent a unique treatment opportunity not only peripheral nervous system disorders but also for selected symptomatic sequelae of central nervous system disorders.

PN 28. Imaging Peripheral Nerve Regeneration Using Serial Section Electron Microscopy: Thinking Like an Axon

Jonathan I Leckenby, MBBS, BSc, MRCS¹; Adriaan O Grobbelaar, MBChB, MMed(Plast.), FCS(SA)(Plast.), FRCS(Plast.)²

¹*University College of London, London, United Kingdom;* ²*The Royal Free Hospital, London, United Kingdom*

Introduction: Peripheral nerve assessment has traditionally been studied through histological and immunological staining techniques in a limited cross-sectional modality. The introduction of transgenic species, such as YFP-H mice, has greatly increased our ability to observe axonal regeneration. However, detailed analysis is still difficult to assess with either of these methods. A new application of serial section electron microscopy (SSEM) is presented to overcome these limitations.

Methods: Direct nerve repairs (DNR) were performed on the posterior auricular nerve of YFP-H mice. Six weeks post-operatively the nerves were imaged using confocal fluorescent microscopy then excised and embedded in resin. Resin blocks were sequentially sectioned at 100nm and sections were serially imaged with an electron microscope (Magellan 400L, FEI). Images were aligned and auto-segmented to allow for 3D reconstruction.

Results: Basic morphometry and axonal counts were fully automated. Using full 3D reconstructions, the relationships between the axons, the Nodes of Ranvier, and Schwann cells could be fully appreciated. The interactions of individual axons with their surrounding environment could be visualised and explored in a virtual environment.

Conclusions: SSEM allows the detailed pathway of the regenerating axon to be visualised in a 3D virtual space. Fully automated histo-morphometry can now give accurate axonal counts and provide information regarding the quality of nerve regeneration. It is possible to fully visualise and ‘fly-through’ the regenerating nerve to help understand the behaviour of an axon with its environment.

PN 29. Electrical Stimulation as a Conditioning Lesion for Peripheral Nerve Regeneration

Jenna-Lynn B Senger, MD; K. Ming Chan, MD; Jaret L Olson, MD; Christine Webber, PhD
University of Alberta, Edmonton, AB, Canada

Introduction. The beneficial effects of a preinjury crush conditioning lesion (CL) on peripheral nerve regeneration have been well-documented in animal models. Despite this, no human studies have been attempted to date. Principle reasons are the ethical dilemma of deliberately injuring an intact nerve and the difficulty in predicting the timing of a nerve injury. Recent studies demonstrated that 1 hour of electrical stimulation (ES) produces effects similar to CL in neuronal cultures, suggesting its role as a clinically translatable conditioning technique to enhance regeneration. This study hypothesizes that ES prior to nerve injury will enhance nerve regeneration.

Materials & Methods. Twelve Sprague-Dawley rats were equally divided into four groups based on conditioning-type to the common peroneal (CP) nerve: ES, crush, sham-ES, and naïve. Three days following conditioning, dorsal root ganglia (DRGs) were collected and stained for growth associated factor-43 (GAP-43), brain-derived neurotrophic factor (BDNF), and glial fibrillary acidic protein (GFAP). A second cohort of 24 animals, one week following conditioning, underwent a cut/coaptation of the CP nerve at the sciatic trifurcation. On post-cut day seven, to determine the extent of axon growth, nerves were collected and stained with NF200 and GFAP.

Results. Three day post-conditioning, DRGs from animals in the ES and crush groups showed significant increase in GAP-43 and BDNF expression compared to sham and naïve ($p < 0.001$). The satellite glial cells in the DRGs from animals in the ES and crush conditioning groups showed a significant increase in GFAP expression (29.3% and 39.3% respectively) compared to sham (8.6%) and naïve (13.5%). Increased RAG expression suggests ES should improve regeneration similar to a crush conditioning. Axonal counts revealed similar lengths of regeneration between ES and crush (4.2 ± 0.6 mm vs. 4.3 ± 0.4 mm, $p = 0.66$) that were superior to sham-stimulation (1.2 ± 0.4 mm, $p < 0.05$) and naïve (1.1 ± 0.3 mm, $p < 0.05$). A greater number of axons at the distal tip were present in animals that received either ES or crush conditioning compared to the unconditioned groups.

Conclusions. By demonstrating similar improvements in axon regeneration, this study suggests that ES conditioning may produce regenerative outcomes comparable to the traditional crush injury model. This opens the possibility of testing ES for conditioning-like effects in clinical trials prior to nerve surgery to enhance nerve regeneration.

PN 30. GDNF Gene Therapy with a Novel Immune-Evasive Gene Switch Promotes Regeneration of Ventral Roots

Ruben Eggers, BSc¹; Fred De Winter, PhD¹; S. a. Hoyng, PhD¹; Martijn JA Malessy, MD, PhD²; Martijn Tannemaat, MD, PhD³; Joost Verhaagen, PhD¹

¹*Neuroregeneration, Netherlands Institute for Neurosciences, Amsterdam, Netherlands;*

²*Department of Neurosurgery, Leiden University Medical Center, Leiden, Netherlands;*

³*University of Leiden, Leiden, Netherlands*

Introduction. In patients lesions of the brachial plexus causes permanent loss of function. After experimental lumbar ventral root avulsion, reimplantation promotes motoneuron survival and a limited degree of axon regeneration. Prolonged, uncontrolled lentiviral vector-mediated expression of glial cell-line derived neurotrophic factor (GDNF) in reimplanted ventral roots enhanced motoneuron survival and axonal outgrowth into the root. Persistent, uncontrolled GDNF expression results in trapping of axons and a failure to reinnervate the hind paw. The goal of the current study was to overcome these adverse effects by exerting temporal control over the expression of GDNF by using a novel immune-evasive gene switch which can be turned on by the antibiotic doxycycline.

Materials and Methods. High titer ($\sim 10^{10}$ gc/ml) lentiviral vectors were produced in HEK cells and applied to L3-L5 ventral roots of adult Wistar rats as previously reported. GDNF expression was regulated in the transduced reimplanted ventral roots using doxycycline-supplemented food for 4 (on/off group, n=14) or 24 weeks (on group, n=14) post-surgery.

Results. A 5 fold increased expression of GDNF for either 4 wk followed by a decline to baseline expression levels, or in persistent expression of GDNF for 12 and 24 wk was detected using a GDNF Elisa. Motoneuron survival was increased in all GDNF treated groups irrespective of the doxycycline treatment period. At the reimplantation site, GDNF induced robust regrowth of regenerating motor fibers into the root. Persistent GDNF expression resulted in coiled fiber growth. The ventral roots exposed to persistent GDNF expression are enlarged in comparison to GFP controls. In contrast, in the 4 wk GDNF group, axons in the ventral root display a longitudinally organized growth pattern and the roots are less enlarged. Biweekly compound muscle action potentials (CMAP) measurements revealed that 4 wk GDNF expression led to an earlier recovery of CMAPs and a significant increase in amplitude compared to animals with persistent GDNF expression and GFP controls. Further histological analysis of axon regeneration revealed a two fold increase in the number of axons in the sciatic nerve at 9 cm from the reimplantation site.

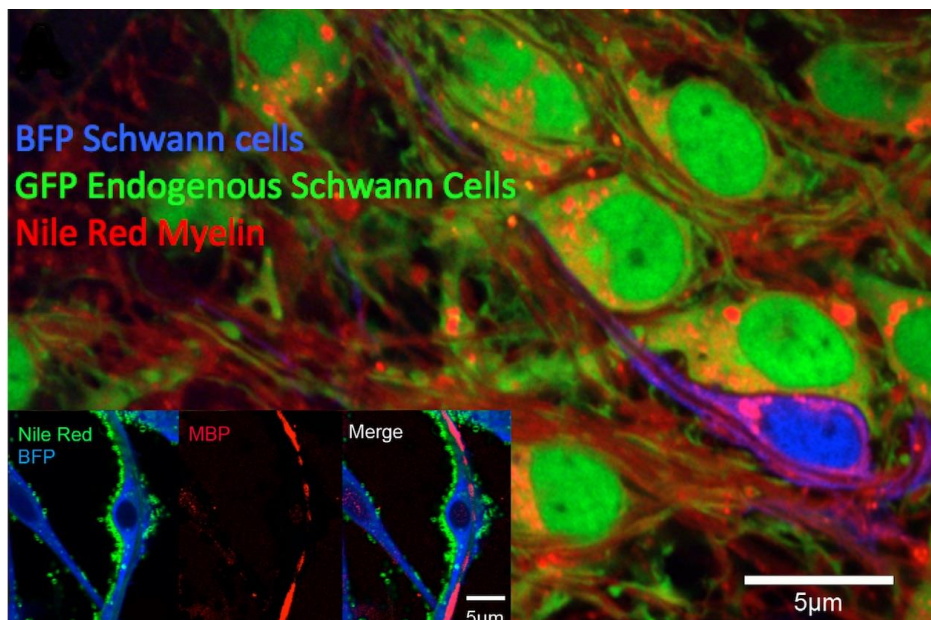
Conclusion. Timed GDNF expression using our novel stealth gene switch in a long distance regeneration model results in enhanced motoneuron survival and reduces local trapping of regenerating motor axons at sites of high GDNF expression. The observed improved CMAP values indicate that timed GDNF expression results in a potentiation of long distance regeneration and muscle innervation.

PN 31. Schwann Cells Transport Lipid Rich Vesicles during In-vitro Myelination as Revealed by Video Lapse Spectral Imaging

Joey Kevin Grochmal, MD, PhD; Raj Midha, MD, MSc

University of Calgary, Calgary, AB, Canada

Introduction: Peripheral nerve myelin synthesis requires a large volume of hydrocarbon molecules to support the exponential production of lipid bilayer inherent in its formation; this provision occurs through a process that is yet unclear. **Methods:** Using spectral confocal microscopy, we studied exogenous BFP expressing Schwann cells as they progressively myelinated in GFP-DRG explant co-cultures (Figure 1: In-vitro myelination by exogenous BFP and endogenous GFP expressing Schwann cells, with myelin labelling by Nile Red. Exogenous Schwann cells produce myelin basic protein -inset).



Noticing lipid-rich Schwann cell domains by staining tissue living cultures with Nile Red, we then used time-lapse imaging to capture retrograde vesicular transport live in-vitro (Figure 2).

Results: Schwann cells are observed to transport lipid-rich vesicles with a spectral signature indicative of extensive cholesterol content, in the context of elongated alignment with DRG neurites (Figure 2- Lipid vesicles in bright yellow, Schwann cell cytoplasm in blue with evident nucleus). These vesicles move in a retrograde fashion (at a speed similar to that of retrograde axonal transport) and appear to coalesce in the perinuclear area, consistent with incorporation into the Golgi and rough endoplasmic reticulum organelles. They also experience sudden changes in velocity, suggesting that these are actively transported vesicles rather than passively diffusing lipid microdomains. **Conclusion:** We provide initial evidence in support of active cytoplasmic transport by Schwann cells of lipid-rich vesicles, a phenomenon that may be a precursor to their use as building blocks in myelination.

PN 32. Ablation of Terminal Schwann Cells after Nerve Injury

Katherine Bernadette Santosa, MD; Albina Jablonka-Shariff, PhD; Alison K. Snyder-Warwick, MD

Washington University School of Medicine, St. Louis, MO

Purpose: Terminal Schwann cells (tSCs) are a special type of supportive glial cells that reside at the neuromuscular junction (NMJ), and are particularly active during reinnervation. After nerve injury, tSCs induce nerve terminal sprouting and extend elaborate processes beyond the NMJ, which help guide regenerating axons. While tSCs are known to support NMJ reinnervation, the requirement of tSCs for and specific contributions to NMJ reinnervation in mammalian species is not known. By ablating tSCs in mice, we sought to determine the role of tSCs on the health of the NMJ after nerve injury.

Methods: Adult *S100-GFP* mice underwent right sciatic nerve transection with repair (t=0). Twenty-four hours later, these mice underwent injection of their right extensor digitorum longus (EDL) muscles with either GD3 anti-disialosyl antibodies to ablate tSCs (i.e. experimental group) or an equivalent volume of Lactated Ringer's (i.e. control group). At t=1 or 6 weeks after the initial nerve injury, animals were sacrificed, and EDL muscles were harvested. We then evaluated NMJ morphology within the EDL utilizing confocal microscopy.

Results: Following tSC ablation with GD3 anti-disialosyl antibodies, the total number of tSCs per NMJ was reduced at 6 weeks following nerve injury compared to controls (3 vs. 2, $p < 0.0001$). In addition to being fewer in number, tSCs present at 6 weeks after injury and tSC ablation exhibited weaker S100 staining intensity than in controls. Endplate fragmentation was notably greater in mice that underwent tSC ablation versus those that received sham injections (52.2% vs. 13.2%).

Conclusions: Our data suggest that we were successfully able to specifically target tSCs in mice using the GD3 anti-disialosyl antibody. Moreover, tSC ablation 24 hours after nerve injury leads to increased fragmentation of endplates, suggesting an important role of tSCs in the health and maintenance of the NMJ following nerve injury and repair. Further investigation is ongoing to determine the importance of tSCs on reinnervation of the NMJ following nerve injury.

PN 33. Interaction of Human Schwann Cells with an Artificial Axon Captured at High Definition

Antonio Merolli, MD, FBSE; Yong Mao, PhD; Joachim Kohn, PhD, FBSE
Rutgers - The State University of New Jersey, Piscataway, NJ

INTRODUCTION: Understanding of myelination-remyelination process is essential to guide tissue engineering for nerve regeneration. In vitro models currently used are limited to cell population studies and had difficulty dissecting individual contributors to the process. In a limited number of reports, engineered fibers have been used to evaluate myelination in the absence of axons in vitro; however, by far, Oligodendrocytes but not Schwann cells have been used. We established a novel model in the absence of axons or neuronal factors to address the contribution of biophysical properties of axonal structure to the myelination process by human Schwann cells (HSCs).

MATERIALS AND METHODS: Our model uses a single carbon fiber (CF), suspended in culture media, to provide an elongated structure of defined diameter with 360-degree of surface available for HSCs cells to wrap around. Poly-Capro-lactone 3D printed scaffolds (n=76) supported the CF in a 24-wells-plate. HSCs (ScienCell Research Laboratories, Carlsbad, CA) were cultured. Live cell tracker (C2925, ThermoFisher) was used to image cells day-by-day and for time-lapse studies. After fixation, scaffolds were incubated with anti-MAG (ab89780 AbCam) and anti-MBP (ab124439 AbCam) antibodies and imaged by fluorescence, confocal, scanning electron and Helium-Ion microscopy (without any coating).

RESULTS: We observed cell attachment, elongation and enwrapment around a fiber over a period of 2 weeks. The single wire construct allowed us to track and image each cell with different modalities. After 2-4 hours of incubation, elongation begins and cytoplasmic prolongations start to spiral round the CF. Expression of myelin basic protein (MBP) was clearly detected; it was associated with the expansion of the cell membrane in a vast surface of the CF.

CONCLUSIONS: This model enabled us to spatially and temporally capture the interaction of human Schwann cells with an artificial axon. The possibility to apply multimodal analysis on each individual cell has never been reported in the past. Imaging by Helium-Ion microscopy is also a new modality and it allowed us to associate morphology at high resolution to functional the features previously identified by fluorescent markers (figure 1). The model is suited for the analysis of natural/artificial molecules and external physical factors (e.g. pulsed electrical current) as possible regulators of myelination by HSCs.

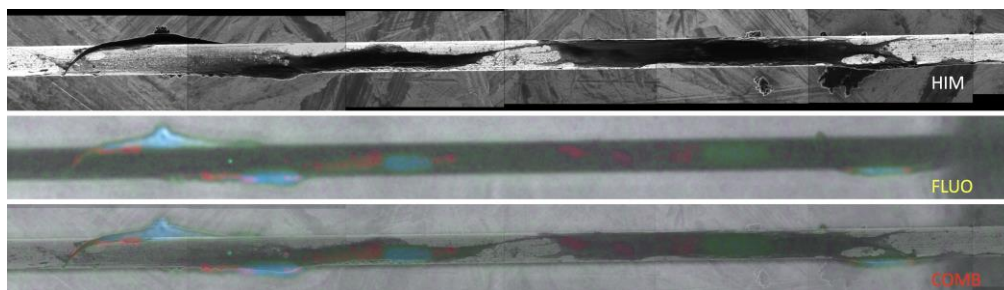


Figure 1. Human Schwann cells culture on a suspended Carbon Fiber of 6.7 micron in diameter: Helium-Ion microscopy at 2200X (HIM); Fluorescence microscopy at 400X (FLUO); combined picture (COMB). (blue=DNA; red=MBP; green=live tracker)

PN 34. Nerve Autograft or Biopsy Related Complications: Evidence-Based Systemic Review

Ivica Ducic, MD, PhD¹; Erick DeVinney, BS²

¹Washington Nerve Institute, McLean, VA; ²AxoGen Inc, Alachua, FL

Introduction: Harvesting nerve autograft or obtaining sensory nerve biopsy for diagnostic purposes is expected to cause permanent sensory deficits. In addition, donor site wound complications; neuroma pain and post-denervational paresthesia may follow, mandating additional treatments due to negative effect on patient's quality of life. Systematic review is undertaken to define the incidence, healthcare cost-related sequels and available solutions for these complications.

Methods: Literature search of available Pub-Med English reported studies was undertaken to address each of the three-targeted goals.

Results: Although various sensory upper and lower extremity nerve donor sites are utilized, sural nerve appears the most common nerve autograft or biopsy donor site. The complication rates for chronic pain (>6months) range from 11-40%, while pain symptoms may persist up to 5 years or more. Diabetic patients have greater risk for chronic post-operative pain (40%, up to 44 months). Allodynia was presented in 19% of patients, while dysesthesia ranged from 35-47%. Donor site wound infection or dehiscence are reported in 3-8% of patients.

The extended operative time for autograft harvest was 30-75 min, with associated OR costs of \$3200-\$6500, and charges for prolonged stay, affected ambulation and pain management. If complication due to surgical site infection, wound dehiscence or neuroma management, healthcare costs can reach \$9700, with \$4-\$22,000 cumulative hospital loses per incidence.

Medical and interventional neuroma management have low long-term success rate as neither removed pain source-neuroma. In addition, overall 55% effectiveness of radiofrequency ablation has high recurrence rate, while about 70% effective neuromodulation appears appealing, only about half are still effective beyond three year, with average of 39% complications. Aside from standard surgical approach, previous reports of modified sural nerve biopsy aimed to minimize donor site complications, still failed to restore the original sensation. While surgical removal of neuroma without reconstruction may have up to 20% of failure rate, reported sensory nerve reconstruction with processed human nerve allograft (*Avance*, AxoGen, FL) is reported to have comparable outcomes to autografts.

Summary: Donor site morbidity due to nerve autograft harvest or diagnostic biopsy may be associated with morbidity and costly complications. The awareness of such events should aid surgeon and patient when choosing nerve autograft vs allograft reconstruction. Newest technologies utilizing human allograft allow donor nerve continuity restoration, thereby eliminating neuroma recurrence, in addition to restoring original nerve function. While technical clinical details will be shared, further prospective studies are suggested to reinforce presented evidence based-data and proposed solutions.

PN 35. FK506 Binding Protein Expression Within the Injured Peripheral Nerve

Kasra Tajdaran, MASc^{1,2}; Jennifer J. Zhang, MD, PhD¹; Tessa Gordon, PhD, DSc¹; Gregory H. Borschel, MD, FAAP, FACS^{1,2}

¹The Hospital for Sick Children, Toronto, ON, Canada; ²University of Toronto, Toronto, ON, Canada

Purpose: The mechanism of action of FK506 on peripheral nerve is still unknown despite the growing interest in local FK506 delivery for enhancing axon regeneration. In this study, we analyzed the expression of FK506-binding proteins (FKBPs), a family of immunophilins that act as receptors for FK506, within the injured peripheral nerve and following local FK506 administration. We investigated the expression of FKBP-12 and FKBP-52 which have been shown to mediate immunosuppressive and neurotrophic properties of FK506 within the central nervous system, respectively.

Methods: Using transgenic *Thy1-GFP+* rats expressing green fluorescent protein (GFP) to visualize peripheral axons, the sciatic nerve was transected and repaired either with or without local FK506 delivery using a particulated FK506 delivery system. In a sham group, the sciatic nerve was not injured. Seven days post repair, immunostaining for FKBPs (FKBP-12 and FKBP-52), Schwann cells (SC; S100), and macrophages (ED-1) was performed to determine the localization and/or co-expression of the proteins within the longitudinal sections of injured and intact sciatic nerve.

Results: With and without FK506 local delivery, FKBP-52 was expressed in SCs in both the proximal and distal stumps adjacent to the site of sciatic nerve injury, 7 days post-repair, as seen in longitudinal nerve sections (**Fig.1**). FK506 delivery promoted an obvious elevation of SC proliferation in the distal nerve stump as compared to the nerves without FK506 delivery. FKBP-52 expression was minimal in the regions of the proximal and distal nerve stumps not adjacent to the injury. FKBP-12 was mainly expressed in the vacuoles of the degenerated nerve fibers in the distal nerve stump, with minimal expression in the proximal nerve and at the site of nerve injury (**Fig.2**). Both FKBP-12 and FKBP52 expression were not detectable within the intact nerves.

Conclusion: The mechanism of action of FK506 on peripheral nerve regeneration has not been completely characterized. Our findings suggest that FK506 acts on the Schwann cells at the site of injury, accounting, at least in part, for the profound enhancement of nerve regeneration when applied locally.

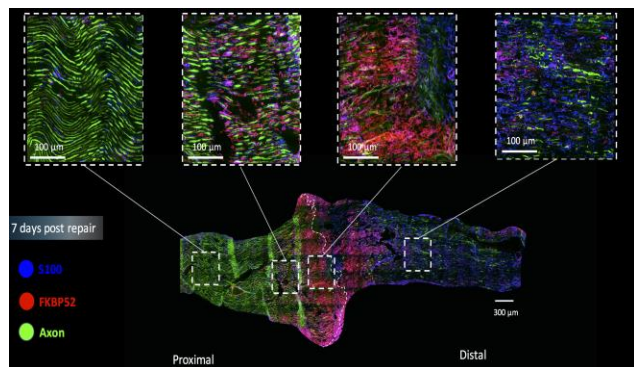


Fig.1. FKBP-52 expression within the injured peripheral nerve.

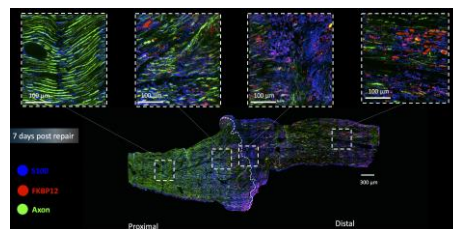


Fig.2. FKBP-12 expression within the injured peripheral nerve.

PN 36. Reinnervation Patterns of Hindlimb Muscle Neuromuscular Junctions after Nerve Injury

Katherine Bernadette Santosa, MD; Bianca Vannucci, BA; Alexandra Marie Keane, BA; Katherine G Campbell, BS; Albina Jablonka-Shariff, PhD; Alison K. Snyder-Warwick, MD
Washington University School of Medicine, St. Louis, MO

Purpose: Several outcome measures to assess nerve regeneration and muscle reinnervation following nerve injury have been described in the literature. Many of these techniques, however, are fraught with limitations such as low sensitivity, need for specialized equipment or mouse lines, and evaluation in an *ex vivo* environment. Here, we present a technique to directly assess motor recovery via confocal microscopic imaging of motor endplate reinnervation. The purpose of our study is to evaluate all neuromuscular junction (NMJ) structures (axon terminals, Schwann cells (SCs), and motor endplates) during hindlimb muscle reinnervation following sciatic nerve transection and repair.

Methods: Adult wildtype (C57BL/6) mice underwent transection of the right sciatic nerve with immediate repair and were randomized to groups corresponding to the time of evaluation (t=0, 1, 2, 3, 4, 8 or 30 weeks) after nerve injury. At the time of harvest, the extensor hallucis longus (EHL) and extensor digitorum longus (EDL) muscles, both innervated by the deep peroneal branch of the sciatic nerve, were collected for whole mount confocal microscopy. NMJ morphology was characterized and reinnervation quantified by imaging axons (NF200), SCs (S100), and motor endplates (α -bungarotoxin).

Results: At one week after sciatic nerve transection and repair, all endplates were denervated. At two weeks, ~54% of endplates were partially innervated. At 3 weeks, nearly 90% of all endplate were at least partially innervated, and NMJs showed evidence of sprouting and polyaxonal reinnervation. At 8 weeks, all endplates were reinnervated, although evidence of sprouting axonal connections between endplates remained. At 30 weeks following injury, single innervation of the NMJ was restored but endplate fragmentation, not seen at earlier time points after nerve injury, was evident.

Conclusions: The abundance of NMJs and the thin muscle bulk of the EHL and EDL make ideal models for evaluation of motor reinnervation following nerve injury. Reinnervation following murine sciatic nerve transection and repair occurs rapidly and is completed by ~3 weeks after injury; however, the normal 1:1 axonal to endplate relationship is not fully restored by 2 months after nerve injury. In the absence of transgenic mouse models whose axons and/or SCs express fluorescent chromophores, we present a consistent and feasible method for evaluating motor reinnervation following nerve injury.

PN 37. Regenerative Sieve Electrodes Induce Sensory Percepts via Electrical Stimulation of Peripheral Nerve Fibers

Matthew R MacEwan, PhD; Juan Pardo, BS; Nikhil Chandra, BS; Daniel W. Moran, PhD; Wilson Z. Ray, MD

Washington University School of Medicine, St. Louis, MO

Introduction: Regenerative sieve electrodes represent a novel means of facilitating chronic high-specificity nerve stimulation needed to restore sensorimotor function following neurological injury. Yet, regenerative sieve electrodes have yet to be proven as a stable interface to sensory nerve fibers capable of inducing actionable sensory percepts. The present study aimed to examine the ability of chronically implanted regenerative sieve electrodes to functionally interface sensory axons in mammalian mixed nerve and exogenously induce cortical signatures of peripheral sensation.

Materials & Methods: Custom-designed sieve electrodes were fabricated out of polyimide and gold using sacrificial photolithography. Regenerative sieve electrodes were then microsurgically implanted in the sciatic nerve of male Lewis rats for 1, 2, and 3 months. Nerve interfacing was assessed in situ by selectively stimulating regenerated nerve tissue via implanted sieve electrodes while simultaneously mapping activation in sensory cortex (S1) utilizing penetrating silicon microelectrodes.

Results: Micro-surgical implantation of sieve electrodes in the sciatic nerve of healthy male rats for 1, 2, and 3 months demonstrated robust axonal regeneration through implanted devices. Sensory mapping demonstrated progressive restoration of sensory on the plantar surface of the paw over 1-3 months. Chronically implanted sieve electrodes demonstrated successful and independent recruitment of sensory nerve fibers and induction of neural activity in somatosensory cortex (S1). Mapping of the sensory cortex (S1) utilizing silicon microelectrode arrays further elucidate the selective nature of sensory fiber activation.

Conclusions: The present study confirms the ability of sieve electrodes to facilitate selective, stable activation of sensory nerve fibers. These findings suggest that regenerative sieve electrodes may be able to provide a stable interface ideal for translational use in advanced neuroprosthetic systems.

PN 38. Rapid Screening Protocol: In Vivo Peripheral Nerve Injury Model for Rapid Screening of Potential Neurotrophic Compounds

Hilton M Kaplan, MBBCh, FCSSA, PhD¹; Wei Chang, PhD¹; Derek J Woloszyn, BS^{1,2}; Matthew Richtmyer, BS¹; Nickolas Rupertus, BS¹; Joachim Kohn, PhD, FBSE¹

¹Rutgers - The State University of New Jersey, Piscataway, NJ; ²Boston University School of Medicine, Boston, MA

INTRODUCTION: Peripheral nerve injuries result in limited recovery, especially over large gaps. Nerve guidance conduits (NGCs) are an attractive option, but prove largely insufficient on their own. Creating a conducive micro-environment by incorporating bioactive moieties to aide speed and accuracy of regeneration, requires lengthy processes (screening, optimizing delivery, in vivo testing), which can take a year or longer. We describe a rapid "pump screening" model that delivers test compounds reliably over 4 weeks, without requiring any special formulation development. At 6 weeks, quantifiable histological outcomes are evaluated, dramatically reducing: study duration (6 vs. 16-24 weeks), animals (by ³75%), and costs (by \pm 68%).

MATERIALS & METHODS:

MODEL: A 1 cm rat sciatic nerve injury is repaired with a tyrosine-derived polycarbonate NGC (1.5 mm ID x 12 mm), with a drug-delivery cannula affixed from a 2 ml Alzet[®] osmotic pump (DURECT, Cupertino, CA) implanted subcutaneously on the back. The pump delivers drug throughout the NGC volume over every 20 hour period for 4 weeks. At 6 weeks samples are assessed histologically.

GROUPS: There are 10 Experimental groups (test compounds that demonstrated promise in vitro, and remain efficacious for 4 weeks at 37 °C); and 4 Control groups: (i) Validation controls using hydrophilic (fluorescein, n=2) and hydrophobic (Nile red, n=2) compounds; (ii) Positive control (BDNF, n=6); (iii) Negative control (No drug, n=6); (iv) Contralateral control (Uninjured nerve, n=6).

HISTOLOGY: Tissues are stained with toluidine blue and osmium tetroxide. Cross-sections (XS) of proximal nerve (3 mm from NGC) and conduit (3 mm into proximal NGC), and longitudinal sections (LS) of the remaining NGC, are assessed for 6 quantifiable parameters: XS = axon count, density, diameter, g-ratio, nerve area; LS = propagation rate.

STATISTICS: Experimental groups are compared to each control group (Tukey test), and to each other (ANOVA), absolutely and for % change from proximal nerve into conduit.

RESULTS: Validation controls demonstrated both hydrophilic and lipophilic compounds were consistently delivered throughout NGCs. Analyses of experimental groups are being completed and will be presented. Currently, one uric acid precursor has demonstrated significant retrograde protection and enhanced sprouting vs. controls ($p < 0.05$).

CONCLUSIONS: We have developed an in vivo model to rapidly screen potentially neurotrophic factors. Major advantages are significant savings in time (avoids months-years formulating slow-release drug delivery platforms for each compound; 6 vs. 16-24 week in vivo studies), animals (6 per group vs. 6 per timepoint = 75+% less); and costs (\pm 68% savings).

Table 1 – Association of Sub-Clinical Peroneal Neuropathy with Falling within a Multivariable Model

History/Exam Findings:	B-coefficient	Fall Odds Ratio [95% CI]	p-value
SCP _N	1.318	3.74 [1.06, 13.14]	0.04
Age (each 1 year increase)	-0.002	0.998 [0.98, 1.02]	0.85
BMI ^(a) (each 1 unit increase)	0.042	1.04 [1.01, 1.08]	0.02
Stairs (1-2 times/week)	-0.668	0.51 [0.21, 1.24]	0.14
Stairs (3+ times/week)	-1.015	0.36 [0.17, 0.78]	<0.01
Plantarflexion Weak (1 leg)	-0.249	0.78 [0.39, 1.54]	0.44
Plantarflexion Weak (both legs)	1.225	3.40 [1.34, 8.66]	0.04
Constant ^(b)	-1.665	0.189	0.05
Nagelkerke R-square – 0.093; Overall Model Significance – p=0.001			
Associations presented as Odds Ratio [95% Confidence Interval] derived from multivariate logistic regression. The effects of walking frequency, alcohol use, anti-hypertensive medications, narcotics, benzodiazepines, balance, gait, vertigo, vision, severe respiratory disease, peripheral neuropathy, and stroke were examined but did not significantly predict within the model. Bold type denotes statistical significance (p<0.05). ^(a) Continuous variable: each 1 unit increase in BMI results in a 4% increase in fall risk. ^(b) Intercept term of regression equation.			

PN 39. Sub-Clinical Peroneal Neuropathy is Common and Associated with Falling in Ambulatory, Community Dwelling Adults

Louis H Poppler, MD, MSCI; Jenny Yu, MD; Susan E. Mackinnon, MD;

Washington University School of Medicine, Saint Louis, MO

Introduction: Peroneal neuropathy with an overt foot drop is a known risk factor for falling. Sub-clinical peroneal neuropathy (SCP_N) due to compression at the fibular head is more subtle and does not have an obvious foot drop. SCP_N was previously found in 31% hospitalized patients and was associated with having fallen. The prevalence of SCP_N among ambulatory outpatients is unknown. Identification and treatment of SCP_N may reduce fall incidence. This study’s purpose is to determine the prevalence of SCP_N in ambulatory outpatients and establish if it is associated with falling.

Methods: A prospective, cross-sectional study of 398 ambulatory outpatients presenting to the plastic and orthopaedic surgical clinics at a large academic tertiary care hospital was performed. Patients referred for peroneal neuropathy were excluded. Patients were examined for findings that suggest peroneal neuropathy, fall risk, and a history of falling. Multivariate logistic regression was used to correlate SCP_N with fall risk (Activity and Balance Confidence (ABC) Scale) and a history of multiple falls in the past year.

Results: The mean age of enrolled patients was 54 ± 15 years and 248 (62%) were female. The population was active with 344 patients (86%) walking more than 30 minutes and 361 (91%) taking a flight of stairs at least one or two times weekly. Thirteen patients (3.3%) were found to have SCP_N. Two patients (0.5%) had bilateral SCP_N. After controlling for various factors known to increase fall risk, patients with SCP_N were 3.74 times [95% confidence interval: 1.06 - 13.14] (p=0.04) more likely to report having fallen multiple times in the past year than patients without SCP_N (Table 1). Similarly, patients with SCP_N were 7.22 times [95% confidence interval: 1.48 - 35.30] (p=0.02) more likely to have an elevated fall risk on the ABC fall risk scale (Table 2). As the number of lower extremities affected increased, the strength of association increased suggesting a cause-effect relationship between SCP_N and falling.

Conclusions: SCP_N is common, affecting 3.3% of ambulatory outpatients, and associated with falling in this active population. Future studies are needed to see if therapy or surgery to treat SCP_N reduce fall incidence in this population.

Table 2 – Association of Sub-Clinical Peroneal Neuropathy and Elevated Fall Risk (ABC Score <67) within a Multivariable Model

History/Exam Findings:	B-coefficient	Fall Odds Ratio [95% CI]	p-value
SCPN	1.977	7.22 [1.48, 35.30]	0.02
Age (each 1 year increase)	0.019	1.07 [0.99, 1.05]	0.23
BMI ^(a) (each 1 unit increase)	0.069	1.07 [1.02, 1.13]	0.01
Stairs (1-2 times/week)	-0.768	0.45 [0.14, 1.52]	0.20
Stairs (3+ times/week)	-1.325	0.27 [0.10, 0.73]	0.01
Plantarflexion Weak (1 leg)	0.922	2.51 [0.99, 6.41]	0.05
Plantarflexion Weak (both legs)	2.947	19.05 [5.67, 63.98]	<0.01
Alcohol (1-2 times/week)	-1.423	0.24 [0.07, 0.79]	0.02
Alcohol (3+ times/week)	-0.550	0.58 [0.17, 1.93]	0.37
Narcotics or Benzodiazepines (1-2 times/week)	0.533	1.70 [0.30, 9.60]	0.55
Narcotics or Benzodiazepines (3+ times/week)	1.183	3.27 [1.23, 8.69]	0.02
Balance	2.578	13.17 [2.73, 63.68]	<0.01
Constant ^(b)	-2.385	0.092	0.15
Nagelkerke R-square – 0.412; Overall Model Significance – p<0.001			
<p>Associations presented as Odds Ratio [95% Confidence Interval] derived from multivariate logistic regression. The effects of walking frequency, anti-hypertensive medications, gait, vertigo, vision, severe respiratory disease, peripheral neuropathy, and stroke were examined but did not significantly predict within the model.</p> <p>Bold type denotes statistical significance (p<0.05).</p> <p>^(a) Continuous variable: each 1 unit increase in BMI results in a 7% increase in fall risk.</p> <p>^(b) Intercept term of regression equation.</p>			

PN 40. Functional Outcomes after Tibial to Peroneal Nerve Transfer in Foot Drop Patients

Matthew WT Curran, MD; Joshua DeSerres, MD; Michael J Morhart, MD, MSc; Jaret L. Olson, MD; K. Ming Chan, MD

University of Alberta, Edmonton, AB, Canada

Purpose: Due to co-activation of antagonistic muscles during gait, functional outcomes following tibial nerve transfer to the tibialis anterior muscle in patients with foot drop have been poor. The purpose of this study was to examine the effects of gait training on functional performance of patients who demonstrated successful reinnervation.

Methods: Using a prospective study design, a consecutive series of patients who underwent tibial nerve transfer to the tibialis anterior muscle were recruited. A terminal motor branch either to the gastrocnemius or toe flexor muscles was used. Once reinnervation was confirmed, the patients either underwent rehab gait training with biofeedback without bracing or used ankle foot orthosis full time. After a minimum of 12 month follow up, differences in ankle dorsiflexion was measured using Stanmore Questionnaire, a functional assessment that includes MRC grades, and quantitative force measurements. Differences between the two groups were compared with non-parametric statistics.

Results: Of the 16 patients who underwent tibial nerve transfer, EMG studies revealed successful reinnervation in 8 [6 males; 36 (22-40) years (median (IQR))]. Five were due to trauma and 3 from oncologic resection. The 5 patients in the rehab training group demonstrated significantly better functional ability as measured by Stanmore [90/100 (65-95) vs 30 (26-41) ($p=0.02$)] compared to 3 in the control group. Patients in the rehab group were able to walk, run and climb stairs without any walking aid. There was no difference in Stanmore scores between different etiologies ($p=0.76$) and donor nerve ($p=0.40$). Force data from patients with above antigravity strength was 25(17-32)% compared to the contralateral side.

Conclusions: Overall the outcomes are mixed. Only 50% of patients had meaningful reinnervation of the tibialis anterior muscle following transfer. In those patients with successful reinnervation, rehab training significantly improved outcomes.

PN 41. Tibial Nerve Compression at the Tarsal Tunnel in both Diabetic and Non-diabetic Subjects

Willem D. Rinkel, MD^{1,2}; Manuel Castro Cabezas, MD, PhD¹; Erwin Birnie, PhD¹; J Henk Coert, MD, PhD^{1,3}

¹*Franciscus Gasthuis & Vlietland, Rotterdam, Netherlands;* ²*Erasmus Medical University Center, Rotterdam, Netherlands;* ³*University Medical center Utrecht, Utrecht, Netherlands*

Introduction: Nerve entrapments like carpal tunnel syndrome are more prevalent in patients with diabetes compared to the general population, especially in those with complaints of diabetic sensorimotor polyneuropathy (DSP). The prevalence of tibial nerve compression at the tarsal tunnel has not been studied extensively yet. Its diagnosis is essential, as therapeutic interventions directed toward relief of entrapment may be effective regardless of the presence of DSP. Our study aim was to determine the prevalence of tibial nerve compression and its associated clinical impairments, in both a diabetic and non-diabetic population.

Materials & Methods: Data of 416 patients (240 non-neuropathic subjects with diabetes and 176 diabetic subjects with neuropathy) participating in the prospective Rotterdam Diabetic Foot Study and 196 reference subjects without diabetes and without neuropathy were evaluated for clinical features of tibial nerve compression at the tarsal tunnel. All subjects underwent sensory testing of the feet and complaints were assessed using the Michigan Neuropathy Screening Instrument.

Results: The prevalence of clinical tibial nerve compression in diabetic patients was 44.9% (CI: 40.1-49.7%) vs. 26.5% (CI: 20.3-32.7%) in healthy controls ($p < .0001$). The prevalence of bilateral compression was higher in diabetic patients with neuropathy complaints (MNSI³⁴) 34.5% (CI: 26.7-42.2%) vs. 23.4% (CI: 17.5-29.2%), $p = .024$). In diabetic patients, unilateral tarsal tunnel syndrome (TTS) was present in 29.9% (CI: 25.2-34.5%), and bilateral TTS in 17.7% (CI: 13.9-21.5%). Significant more neuropathic symptoms ($p < .002$) and higher sensory thresholds were observed in tibial nerve innervated areas, when compressed.

Conclusions: Tibial nerve compression is prevalent in both diabetic subjects and controls. The significant more frequently reported neuropathic complaints and concomitant sensory disturbances suggests a role for super-imposed entrapment neuropathy in diabetes related neuropathy.

PN 42. Targeted Muscle Reinnervation in Upper Extremity Spare-Parts Surgery

Michael T Larsen, MD, MPH¹; Kyle R Eberlin, MD²; John Byers Bowen, MD, MS³; Ian L. Valerio, MD¹

¹*Department of Plastic and Reconstructive Surgery, Columbus, OH;* ²*Massachusetts General Hospital/Harvard Medical School, Boston, MA;* ³*The Ohio State University Wexner Medical Center, Columbus, OH*

Introduction: Targeted muscle reinnervation (TMR) is a relatively recent technique which opens up the possibility for an amputee to operate a myoelectric prosthesis through neural control by coapting severed nerves to alternate muscle recipient sites. Furthermore, this technique shows much promise in decreasing neuroma and phantom limb pain. However, in some extremity amputations, especially fore-quarter amputations, there may be no nearby recipient muscle sites, or the residual nerve may be too short to perform TMR. Using spare-parts from the amputated limb can help solve this problem by providing nerve autograft or by bringing muscle recipient sites more proximal. This study examines techniques and outcomes for spare-parts TMR in upper extremity amputees.

Methods: A retrospective review of all patients that underwent spare-parts TMR between 2016-2017 at two institutions, was performed. Intraoperatively, the proximal stumps of the amputated nerves were identified. A nerve stimulator was used to identify motor nerve branches entering specific muscle sites. These target motor nerves were divided near their entrance into the muscle, and where possible, the proximal stumps of the amputated nerves were then coapting to them. When the proximal nerves were too short, median and/or ulnar nerve was harvested from the amputated limb and used as reverse autograft to span the gap. When amputation resulted in a large soft tissue defect, a spare-parts free flap was used for reconstruction and TMR was performed to target motor nerves in the free flap. Patients are followed to assess for neuroma and phantom limb pain, patient satisfaction, and function.

Results: Five patients have undergone spare-parts TMR. One patient has been lost to follow up. None of the other patients are currently experiencing neuroma or phantom limb pain. A trend toward decreased narcotic use was noted. The patient with the longest follow up, who is six months status post TMR, demonstrates intuitive control of targeted muscles and is being fit for an insurance-approved myoelectric prosthesis.

Conclusion: Our study shows that TMR with eventual neurotization can successfully be performed in amputations without nearby target muscles by using the spare-parts technique. Our results support other published data which show that TMR may decrease the incidence of neuroma and phantom limb pain, and we show that this can be done with nerve autograft or free flap target muscles.

PN 43. Functional Characterization of Mixed, Motor, and Sensory Nerve Regenerative Peripheral Nerve Interfaces (RPNI)

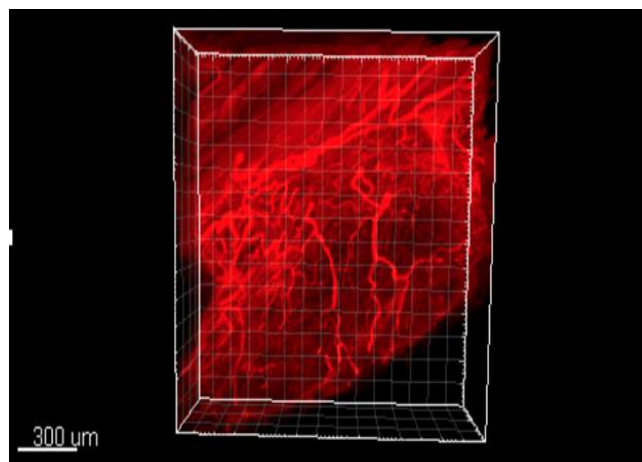
Andrej Nedic, BSc; Alixandra L VanBelkum, BA; Nathan G Lawera, BS; Vincent Thieu, BSc; Zaid Khatib, BSc; Melanie G. Urbanchek, PhD; Paul S Cederna, MD; Stephen W. P. Kemp, PhD, MSc

University of Michigan, Ann Arbor, MI

PURPOSE: Approximately 185,000 Americans suffer devastating limb loss yearly, resulting in substantial functional deficits adversely impacting quality of life. Regenerative Peripheral Nerve Interfaces (RPNI) present a promising surgical strategy for interfacing human volition with myoelectric prostheses. Rat studies led to proof of RPNI long-term function and high signal to noise ratio with no adverse biological effects. However, characterization of different types of nerve RPNI has not yet been evaluated.

MATERIALS AND METHODS: RPNI consisted of a small, autologous partial muscle graft reinnervated by a transected peripheral nerve branch. Five experimental groups were analyzed: (1) Motor (femoral nerve, motor branch) RPNI; (2) Sensory (sural nerve) RPNI; (3) Mixed (common peroneal nerve) RPNI; (4) negative control (common peroneal nerve transected and not repaired), and; (5) positive control (surgical naïve animal). After 3 months of convalescence, terminal EMG measurements were assessed including nerve conduction velocity and compound muscle action potentials (CMAPs). A 5 mm segment proximal to the rpni was harvested and processed for nerve histomorphometry. All RPNI constructs were harvested and processed for Immuno-enabled Three-Dimensional Imaging of Solvent-Cleared Organs (IDISCO) to visualize axonal infiltration into the RPNI. Retrograde labeling was conducted in a separate cohort of animals to determine neuronal numbers innervating individual RPNI.

RESULTS: At harvest, all RPNI were well vascularized but smaller in size than when implanted. Nerve conduction velocities and CMAPs were achieved in all three experimental RPNI groups, with mixed nerve and femoral nerve RPNI displaying greater CMAPs and terminal weights than sensory RPNI. IDISCO revealed the extensive 3-dimensional patterns of axonal reinnervation of each corresponding RPNI (Fig.1). Retrograde labeling showed differences in neuronal numbers between different RPNI groups.



muscle graft.

CONCLUSIONS: Motor, sensory, and mixed nerve RPNI displayed robust neural regeneration. Results from this study will enable us to further evaluate electrode-biological interfaces, and help us develop future prostheses with the ability to respond to both motor and sensory neural signals.

Figure 1. Three-dimensional IDISCO imaging of RPNI shows robust reinnervation of tissues by nerve of varying size. Fluorescent labeling of neurofilament-M (red) shows that peripheral nerve fibers regenerate diffusely throughout the entire free

PN 44. Anatomical and Electrophysiological Analysis of the Mouse Infraorbital Nerve as a Neural Interface

WeiFeng Zeng, MD; Aaron M. Dingle, PhD; Conner Feldman, BS; Jared P Ness, MS; Joseph R. Novello, MS; Mark Austin, UG; Sarah K. Brodnick, BS; Jane Pisaniello, BS; Jacqueline S. Israel, MD; Aaron J Suminski, PhD; Wendell B Lake, MD; Justin C. Williams, PhD; Samuel O. Poore, MD, PhD

University of Wisconsin, Madison, Madison, WI

Introduction: The trigeminal nerve is the fifth cranial nerve, which divides into three branches: ophthalmic (V1), maxillary (V2) and mandibular (V3), and carries most of the tactile, proprioceptive and nociceptive information from the face to the central nervous system (CNS).

The latest preclinical and clinical data indicates that electrical stimulation of the V1 branch treats a variety of neurologic and psychiatric disorders of the CNS (i.e. epilepsy, depression, attention deficit hyperactivity disorder and traumatic brain injury). Despite positive preliminary results in humans, the mechanisms and potential side effects remain largely unknown.

This study applies microsurgical technique to investigate trigeminal nerve interfacing in mice. We describe the development and evaluation of a mouse model of trigeminal nerve stimulation for future mechanistic studies.

Materials and Methods: The trigeminal nerve and its branches was mapped via microsurgical anatomical dissection in mice cadavers. Acute experiments utilized a whisker puffer generate the physiological response in the barrel cortex. Electrical stimulation of the infraorbital nerve was performed distal to the infraorbital foramen with a custom bipolar cuff electrode to replicate the physiological response. Electrical stimulation of the infraorbital nerve was performed using single, monophasic or biphasic (cathode leading) pulses (50-800uA, 100-300us per phase) initiated at pseudorandom intervals (varying between 3-4 seconds). Changes in cortical activity in the barrel cortex were recorded (somatosensory evoked potentials [SSEPs]) custom 16 channel uECoG array.

Results: Investigation of the trigeminal nerve and its branches identified the infraorbital branch as the best candidate for electrical stimulation in mice, measuring 1.6mm in width, 3.2mm in available length, and 2.8mm away from the skin surface. By comparison, the supraorbital branch measured 0.15mm width and 3mm available length. Dorsal and medial access to the infraorbital branch avoids interference with the facial nerve and provides substantial soft tissue to protect the electrode. The magnitude of SSEPs increased monotonically until saturation with increases in stimulation current and activation thresholds decreased with increases in phase duration.

Conclusions: These preliminary results suggest that an infraorbital nerve interface is the best candidate for examining the neural mechanisms of trigeminal nerve stimulation in the mouse. Furthermore, we found every whisker was supplied by individual nerve fiber of the infraorbital nerve, capable of generating a signal in precise areas of cortex dependent on the fiber activated. We are now investigating this model of sensory feedback in the human extremity, a critical component for ideal prosthetic control.

PN 45. Macrophages are Integral to Neuromuscular Junction Reinnervation after Nerve Injury

Katherine Bernadette Santosa, MD; Alexandra Marie Keane, BA; Bianca Vannucci, BA; Albina Jablonka-Shariff, PhD; Alison K. Snyder-Warwick, MD
Washington University School of Medicine, St. Louis, MO

Purpose: Macrophages are well-known for their role in Wallerian degeneration following a nerve injury. Recent studies, however, have suggested additional macrophage roles such as response to hypoxia and angiogenesis propagation, both of which are necessary for nerve regeneration across an injury site. We hypothesize that similar mechanisms occur at the neuromuscular junction (NMJ), and we have previously shown that macrophages are not only recruited to the site of nerve injury, but also to the NMJ and end-target muscle after nerve injury. By utilizing *Ccr2*^{-/-} mice, which have markedly impaired recruitment of macrophages to sites of inflammation and injury, we sought to determine the importance of recruited macrophages to the NMJ on reinnervation following peripheral nerve injury.

Methods: We performed right sciatic nerve transections with immediate repairs on adult wildtype (C57BL/6) and *Ccr2*^{-/-} mice. At two and three weeks following nerve injury, mice from both groups were sacrificed for collection and evaluation of extensor hallucis longus (EHL) and extensor digitorum longus (EDL) muscles. Using whole mount confocal microscopy, we characterized the morphology of the NMJ and quantified reinnervation by imaging axons (NF200), Schwann cells (SCs, S100), and motor endplates (α -bungarotoxin).

Results: At homeostasis, there were no morphological differences in the appearance of the NMJs of wildtype versus *Ccr2*^{-/-} mice. At two weeks after injury, however, we observed more denervated endplates in *Ccr2*^{-/-} mice than in wildtype mice (68.1% vs. 45.4%, $p=0.016$). Similarly, at three weeks after nerve injury, more denervated endplates remained in *Ccr2*^{-/-} mice as compared to age-matched wildtype controls (26.2% vs. 7.3%, $p=0.0043$).

Conclusions: Successful reinnervation of the NMJ following nerve injury is complex and multifaceted. Our data demonstrate that *Ccr2*^{-/-} mice, which have impaired monocyte-derived macrophage recruitment, have delayed reinnervation as compared to age-matched wildtype controls. These results suggest that macrophages are important for reinnervation of the NMJ following peripheral nerve injury. Further investigations to determine the functional consequences of the differences in reinnervation between the two groups are ongoing.

PN 46. Laminin Inhibition to Assess the Regenerative Potential of Peripheral Nerve Allografts

Kasra Tajdaran, MS, Sc; Jennifer Faleris, BS; Mark Friedman, PhD; Erick DeVinney, BS
AxoGen, Alachua, FL

Introduction: Nerve processing methods have been shown to affect structural and biological activity of tissue. Previous studies have demonstrated that preservation of native extracellular matrix (ECM) structure improves the regenerative potential of processed nerve allografts (PNAs). Whilst the activity of basement membrane ECM proteins is known to promote nerve regeneration and contribute to the structure of the endoneurial tubes, their role has not been investigated in PNAs. To evaluate the necessity of maintaining these proteins, a three-dimensional *in vitro* assay was developed. The PNA's regenerative capacity after treatment with functional blocking antibodies of laminin and collagen IV was analyzed via axonal outgrowth measurement. Basement membrane blocking was performed while maintaining the native ECM architecture.

Methods: All PNA samples were pre-treated as according to Table 1 Experimental Design. After pre-treatment, a rat DRG was secured on the end of each PNA with a thin collagen gel. Samples were then cultured for 7 days at 37 °C and 5% CO₂. All samples were longitudinally sectioned and stained with βIII-Tubulin. The neurite outgrowth length was measured, and the three longest neurites in each sample were reported and averaged.

Group ID	Description	Laminin Monoclonal Antibody				
		4C7	4E10	3E5	Collagen IV Antibody	Formaldehyde
L2	Laminin Abs (2 µg/mL)	✓	✓	✓	-	-
L20	Laminin Abs (20 µg/mL)	✓	✓	✓	-	-
L2F	Laminin Abs (2 µg/mL) With Formaldehyde Treatment	✓	✓	✓	-	✓
L20F	Laminin Abs (20 µg/mL) With Formaldehyde Treatment	✓	✓	✓	-	✓
LC20F	Laminin Abs + Collagen IV Ab (20 µg/mL) With Formaldehyde Treatment	✓	✓	✓	✓	✓
F	Formaldehyde Treatment	-	-	-	-	✓
P	Positive Control	-	-	-	-	-

Table 1. Experimental Design

Results: Formaldehyde treatment was necessary to prevent antibody dissociation as shown in groups L2F, L20F and LC20F, which resulted in significantly reduced neurite outgrowth compared to the P group ($p < 0.001$). Comparatively, antibody only treatment groups, L2 and L20, exhibited similar neurite extension compared to group P. The amount of neurite outgrowth was not affected by the laminin antibody concentrations or the addition of collagen IV antibodies in this study, which requires further investigation regarding dose dependence.

Conclusion: The assay utilized in this study provides a valuable technique for isolating the effects of laminin and Collagen IV on neurite outgrowth through PNAs. Previous studies have suggested the importance of microarchitecture for the maintenance of neurite outgrowth in PNAs. This study confirms that functionality of proteins within the basement membrane, specifically laminin, are a key mechanism of action for neurite outgrowth through PNAs. Neurite extension was significantly inhibited by functionally blocking a single component of the basement membrane, laminin, within the intact architecture of the PNAs. As different tissue processing methodologies can alter the activity of the constituent proteins, activity assessments should be performed to understand the effects of processing on the regenerative potential of PNAs.

PN 47. Clinical Outcomes of Nerve Transfers in Patients with Peroneal Nerve Palsy: A Systematic Review and Meta-Analysis

Linden Kyle Head, MD, HBA, BSc, BPHE; Katie Hicks, BSc; Gerald Wolff, BSc, MD, FRCPC; Kirsty Usher Boyd, MD, FRCSC
University of Ottawa, Ottawa, ON, Canada

INTRODUCTION: Peroneal nerve palsy and its associated foot drop is typically managed with ankle-foot orthosis, autogenous nerve grafting, or tendon transfers. Nerve transfers have the potential to reestablish ankle dorsiflexion in this patient population. The objective of this study was to review the clinical outcomes of nerve transfers in patients with peroneal nerve palsy.

MATERIALS & METHODS: Review methodology was registered with PROSPERO and the Preferred Reporting Items for Systematic Reviews and Meta-Analyses (PRISMA) guidelines were followed. A systematic search of MEDLINE, EMBASE, and The Cochrane Library was conducted. English studies were included that investigated the clinical outcomes of nerve transfers in patients with peroneal nerve palsy. Two independent reviewers performed screening and data extraction. Methodological quality was evaluated using the Newcastle-Ottawa Scale (NOS) for assessing non-randomized studies in meta-analyses. Meta-analysis of pooled data was performed using descriptive statistics, Kruskal-Wallis test, and Spearman's rho.

RESULTS: Systematic literature search identified 106 unique articles. Following screening, 12 full-text articles were reviewed and 4 met inclusion criteria for data extraction, qualitative synthesis, and meta-analysis. All included studies were retrospective case series with a mean NOS score of 5.0/6.0. In total, 41 patients underwent nerve transfers for peroneal nerve palsy – mean age of 36.1 years (range=15.0-73.0), mean time to surgery of 6.3 months (range=2.0-12.0), and a mean follow-up of 19.0 months (range=6.0-36.0). Etiology of peroneal nerve palsy was variable: common/deep peroneal nerve injury (n=25, 61%), sciatic nerve injury (n=12, 29%), and lumbar root/plexus injury (n=4, 10%). The donor nerve was either tibial nerve branches/fascicles (n=36, 88%) or the superficial peroneal nerve (n=5, 12%). The recipient nerve was either the deep peroneal nerve (n=24, 59%) or the branch to tibialis anterior (n=17, 41%). Mean postoperative ankle dorsiflexion strength was Medical Research Council (MRC) 2.1 (SD=1.8) with the following distribution: MRC 0 (n=14, 34%), MRC 1 (n=4, 10%), MRC 2 (n=2, 5%), MRC 3 (n=6, 15%), MRC 4 (n=15, 37%), MRC 5 (n=0, 0%). There were no significant differences in ankle dorsiflexion strength between etiologies (p=0.491), donor (p=0.066), or recipient nerves (p=0.496). There were no significant correlations between ankle dorsiflexion strength and patient age (p=0.094) or time to surgery (p=0.493).

CONCLUSIONS: The literature exploring the outcomes of nerve transfers in patients with peroneal nerve palsy is sparse: there are no comparative studies and the retrospective series demonstrate wide variability in outcomes. Further investigations are required to better elucidate the role for nerve transfers in peroneal nerve palsy.

PN 48. Using DTI MRI to Predict Peripheral Nerve Recovery in a Rat Sciatic Nerve Model

Marlieke Nussenbaum, MD; Angel Farinas, MD; Isaac Mazanera Esteve, PhD; Alonda Pollins, MLI; Nancy Cardwell, BS; Richard Dortch, PhD; Wesley Thayer, MD, PhD

Vanderbilt University Medical Center, Nashville, TN

Introduction Peripheral nerve transection is a common injury, with single cut nerve lacerations accounting for over 60% of peripheral nerve surgical interventions in recent studies. For recovery to occur in these patients, axons must grow from the site of repair to the target tissues, a length of up to a meter in humans. Currently, clinical examination and electrodiagnostic tests are the standard practice for peripheral nerve assessment; however neither can rapidly predict whether function will be regained. By the time a diagnosis is made, revisional surgery may not be a viable option due to the onset of irreversible muscle atrophy. Diffusion tensor imaging (DTI) is an MRI sequence that leverages the anisotropic diffusion of water molecules through axons to aid in visualization of neural tracts. DTI parameters, such as fractional anisotropy (FA) and mean diffusivity (MD) are able to quantify microstructural characteristics of nerves, such as axon density and myelin thickness.

Methods Forty eight female Sprague-Dawley rats were divided into two groups and a sciatic nerve injury model was used. Half of the rats underwent complete nerve transection and immediate microsurgical repair; the other half underwent dissection and exposure of the nerve with no nerve injury (control). Behavioral testing (foot fault and sciatic function index) was performed weekly and the nerves were harvested at 4 different time points: 1 week, 2 weeks, 4 weeks, and 12 weeks, and sent for DTI MRI and subsequent toluidine blue staining for axon counts.

Results The mean fractional anisotropy of the imaged nerves were calculated for each time point in both the region proximal and distal to the site of injury and repair (Figure 1), with the proximal region showing trends very similar to the control group while the distal region shows a slow increase which mimics results of behavioral testing. Representative fiber tracking based on MRI parameters is shown in Figure 2.

Conclusion DTI MRI parameters show promise in imaging peripheral nerve injury as well as tracking regain of function following repair.

Figure 1

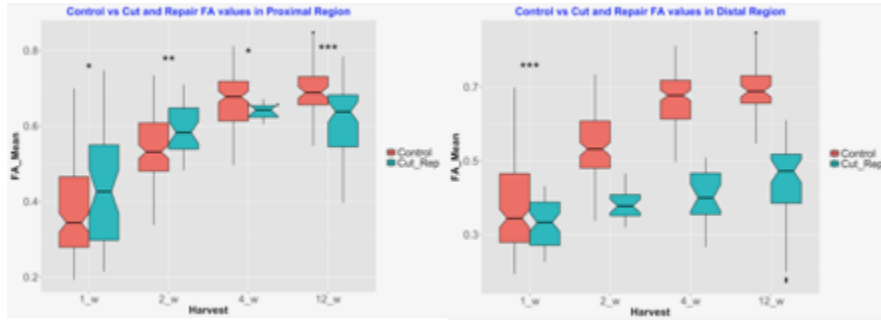
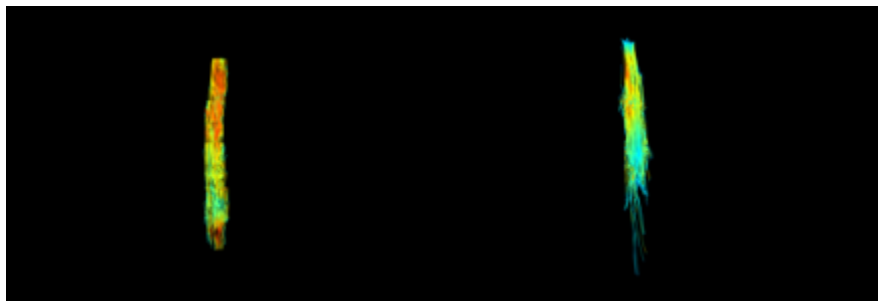


Figure 2



PN 49. Age-related shift of Wallerian degeneration after peripheral nerve injury

Zhongyu Li, MD, PhD; Tiefu Liu, PhD; Thomas L. Smith, PhD; Jiaozhong Cai, BS
Wake Forest School of Medicine, Winston-Salem, NC

Introduction: It is well known that age natively influence peripheral nerve regeneration after injury, however, the underlining molecular mechanisms remain unclear. Wallerian degeneration is the essential part of the nerve regeneration by attracting and activating macrophages to clear myelin debris. This study tested the hypothesis that inflammatory response to nerve injury decreases with age resulting in delayed and/or decreased macrophage recruitment and activation, and therefore limiting axonal regrowth.

Material & Methods: In 15 young (2 months) and 15 adult (12 months) Lewis rats, unilateral sciatic nerve crush injury was induced. Both sciatic nerves from each animal were harvested at one, three, and ten days after injury. Immunohistochemistry was performed for MCP-1, ED-1, CD14 & CD68 and qRT-PCR was done using Taqman (Applied Biosystems) for MCP-1, TNF- α and IL-10 as target genes and Glyceraldehyde 3-phosphate dehydrogenase (GAPDH) as endogenous control. Two-way ANOVA was used for analysis the effect of age on the overall gene expression.

Results: Young animals showed significantly earlier (started on day 1 and maintained through day 10) and stronger MCP-1 and TNF- α expression than adults animals ($P < 0.01$, Figure 1). In contrast, adult animals had stronger expression of IL-10 after crush injury. This delayed and weaker proinflammatory cytokine expression correlated with delaying in nuclear count increases and recruitment of homogeneous macrophages (ED1 positive).

Conclusion

The significant reduction and delay of inflammatory cytokine expression and macrophage recruitment in adult animals after nerve injury indicates that age negatively impacts the rate of myelin clearance during Wallerian degeneration. This age-related shift in Wallerian degeneration may be in part contributing to the decline of nerve regeneration potential in adults.

PN 50. Tissue Engineering Strategies to Bridge Segmental Defects and Maintain Distal Target Efficacy Following Major Peripheral Nerve Injury

Zarina S Ali, MD; Justin C Burrell, MS; Suradip Das, PhD; Kritika S. Katiyar, BS; Kevin D Browne, BS; D. Kacy Cullen, PhD

University of Pennsylvania, Philadelphia, PA

Peripheral nerve injury (PNI) is a common affliction that affects individuals of all age groups and socioeconomic backgrounds. Even following state-of-the-art surgical reconstruction, patients face a high probability of residual functional deficits – especially when axons are tasked with regenerating over long distances that require many months to reach distal targets. To address this need, our research team is pioneering the first dual peripheral nerve repair strategy that provides tissue engineered living “bridges” across missing nerve segments while maintaining the full regenerative pathway and capacity for target muscle reinnervation – a phenomenon we refer to as “babysitting”. For bridging, we have developed tissue engineered nerve grafts (TENGS), which are lab-grown constructs consisting of aligned axonal tracts that we routinely generate in custom-built mechanobioreactors at densities of $>100,000$ axons and lengths of ≥ 5 cm within 2 weeks through the controlled process of axon “stretch-growth”. TENG axons mimic the developmental action of pioneer axons, where targeted axonal outgrowth can be achieved along pre-existing axonal tracts *in vivo*. Indeed, we have shown that TENGS effectively serve as a bridge across segmental nerve defects by accelerating and directing axonal regeneration in rat and pig models of PNI. In the pig, TENG-based repair of a major gap (5cm) in a critical motor nerve resulted in significant reinnervation of distant end targets (>18 cm from lesion). For babysitting, we have implanted separate miniature TENGS – comprised of motor and sensory neurons – within the otherwise denervated distal nerve sheath, which extend axons to integrate with host Schwann cells and target muscle to thereby maintain pro-regenerative capacity and increase the window for long distance axonal regeneration and reinnervation. Using our established porcine model of major PNI, we are assessing the simultaneous ability of bridging TENGS to accelerate axonal regeneration across the zone of injury while employing separate babysitting TENGS to sustain the regenerative environment of distal Schwann cells and receptiveness of target muscles to enable host axons to reinnervate ultra long-distance targets. This dual regenerative medicine strategy may accelerate axonal regeneration while maintaining the structure and function of denervated muscle and sensory end targets to allow functional reinnervation following currently intractable PNI. This work is supported by the U.S. Dept. of Defense (W81XWH-15-1-0466 & W81XWH-16-1-0796).

PN 203 SIRT1 Inhibition Improves Age-related Shift in Wallerian Degeneration

Zhongyu Li, MD, PhD¹; Tiefu Liu, PhD²; Jiaozhong Cai, BS²; Thomas L. Smith, PhD²

¹Wake Forest Baptist Medical Center, Winston-Salem, NC; ²Wake Forest School of Medicine, Winston-Salem, NC

Introduction: The underlying molecular mechanisms of poor neurologic recovery after peripheral nerve injury in adults remain unclear. Cellular energy NAD⁺-dependent SIRT1 deacetylase coordinates Wallerian degeneration (WD) after peripheral nerve injury by reprogramming immunometabolic genes and posttranslational modifications of signal proteins and metabolic key enzymes. We hypothesize that age-associated shift in Wallerian degeneration is SIRT1 dependent, pharmacological inhibition of SIRT1 acutely after peripheral nerve injury may improve Wallerian degeneration process in adult animals.

Material & Methods: Sciatic nerve crush model was produced in young (2-month old) and adult (12-month old) Lewis rats. Sciatic nerve samples were harvested at 1, 3 or 10 days after crush and continuous sections distal to the marked injury site were made for histology and immunohistochemistry studies. Inflammatory gene expression of sciatic nerve tissues were analyzed using qRT-PCR. The effect of NAD⁺ downstream effector SIRT1 on WD generation was studied by administering SIRT1 specific inhibitor EX-527 or vehicle after nerve crush injury.

Results: In contrast to young animals, adult rats displayed an initial immune suppressive response after axonal crush with attenuated expression of pro-inflammatory genes (TNF- α , MCP-1) and delayed recruitment and activation of hematogenous macrophages. These modifications of WD in adult animals were positively correlated with baseline axonal expression of SIRT1. Pharmacological inhibition of SIRT1 by EX-527 restores pro-inflammatory MCP-1 gene expression (Figure 1).

Conclusion: Aging alters the process of WD after peripheral nerve injury. Inhibition of SIRT1 improves WD. Rejuvenation of WD by modulating SIRT1 activity could be a potential adjunct therapeutic strategy for the treatment of peripheral nerve injury in adult patients.

PN 204 Extracting Regenerative Peripheral Nerve Interface Signals from Human Subjects for Neuroprosthetic control

Carrie A Kubiak, MD; Philip Vu, MSE; Zachary T Irwin, PhD; Chrono Nu, BSc; Troy Henning, MD; Deanna Gates, PhD; RB Gillespie, PhD; Theodore A. Kung, MD; Paul S. Cederna, MD; Cynthia Chestek, PhD; Stephen W. P. Kemp, PhD, MSc
University of Michigan, Ann Arbor, MI

Introduction: Peripheral nerves provide a promising source for neuroprosthetic control given their functional selectivity and relative ease of accessibility. However, current interface methods, such as penetrating electrodes, are limited in a clinical setting either by low signal amplitude or interface instability. Here, we address these issues by extracting hand level prosthetic control signals from Regenerative Peripheral Nerve Interfaces (RPNI) implanted within 3 human subjects.

Materials and Methods: RPNIs are constructed by suturing a graft of devascularized, denervated muscle to the residual end of a severed nerve. The graft then revascularizes, regenerates and becomes reinnervated by the transected nerve, creating a stable bioamplifier that produces recordable electromyography (EMG) signals. In addition, nerves can be surgically subdivided into individual fascicles to construct multiple RPNIs and independent signal sources. Here, 2 distal transradial (P1, P2) and 1 proximal transradial (P3) amputees were implanted with RPNIs. P1 and P2 were each implanted with 3 RPNIs with a single graft placed on each of the median, ulnar, and dorsal radial sensory nerve. P3 had 9 RPNIs implanted, with the median, ulnar, and radial nerves subdivided into 4, 3, and 2 branches, respectively. During acute recording sessions, we used ultrasound to locate and implant percutaneous fine-wire bipolar electrodes within the RPNIs. When available, relevant finger-related residual muscles were also implanted with control electrodes. A total of 3-8 electrodes were inserted per recording session.

Results: P1 and P2 produced EMG signals within a range of 20-270 μ Vp-p from the median RPNI, with a signal-to-noise ratio (SNR) between 2.2-31.4 and 50-140 μ Vp-p from the ulnar RPNI with a SNR between 3.3-11.6. P3's 3 ulnar RPNIs produced signals with a range of 30-50 μ Vp-p and SNR of 1.6-5.6, and the 2 radial RPNIs produced signals with a range of 14.5-28.3 μ Vp-p and SNR of 2.0-3.0. Using a combination of RPNI and residual muscle signals, subjects successfully controlled a virtual prosthesis in real-time. For P1, a Naïve Bayes classifier was able to classify movements as either rest, index, middle, or thumb opposition in a 212-trial session with 96.2% accuracy using temporal features of the EMG waveform within 300-1500Hz and binned at 50ms. Similarly, P2 could control rest, thumb, or index with 100% accuracy in a 115-trial session, while P3 could control between little and fist movements with 96.2% accuracy.

Conclusions: Overall, we have demonstrated that RPNIs may provide a clinically viable strategy for producing high amplitude signals from severed nerves for neuroprosthetic control.

PN 103. WITHDRAWN



PN 104. Cross-Cross Sensory Nerve Grafts to Enhance Sensory Recovery in Complex Ulnar Neuropathy

John M Felder, MD; Hollie Power, MD; Elspeth Hill, MD; Jessica Hasak, RN; Susan E. Mackinnon, MD

Washington University, St Louis, MO

Introduction: Debilitating sensory loss is a prominent feature of severe ulnar neuropathy with few surgical options proposed to improve recovery. Here we report our experience with side-to-side sensory nerve grafting from the median to ulnar nerve (cross-cross grafts) to enhance sensory recovery.

Methods: Cross-cross nerve grafting involves tension-free grafting from the sensory component of the median

nerve to the sensory component of the ulnar nerve, in the palm, in a side-to-side fashion, employing short segment allo or autograft.

A retrospective chart review was performed to identifying patients with severe ulnar neuropathy who underwent cross-cross nerve grafting to enhance sensory. Patients were included if they had objective loss of protective sensation in the ulnar distribution with 2-point discrimination $>8\text{mm}$, Semmes-Weinstein monofilament testing (SWMT) >4.56 or no sensory response on nerve conduction testing. These patients underwent cross-cross nerve grafting from the sensory component of the median nerve to the sensory component of the ulnar nerve in the palm. Analysis included assessment of patient aetiology, procedures, nerve conduction studies, objective sensory testing and DASH disability score.

Results: 48 patients underwent cross-cross nerve grafting at our institution between 2014-2017. Of these, 20 patients had severe cubital tunnel syndrome, 7 had brachial plexus injury, 4 had ulnar nerve lacerations and 2 cervical radiculopathies. Of the patients with cubital tunnel syndrome, 60% were revisionary cases. 33 patients had anterior transposition of the ulnar nerve at the elbow and 32 also had a supercharged end-to-side AIN to ulnar nerve transfer. 24 patients had documented loss of ulnar protective sensation or 2 point discrimination $>8\text{ mm}$ pre-operatively, and had adequate follow up for inclusion. 21 out of 24 patients (87%) had return of protective sensation within 1 year as assessed by SWMT and/or 2-point discrimination. DASH disability scores improved significantly. Technique and case examples are presented.

Conclusions: Cross-cross nerve grafting may be a useful adjunct to enhance sensory recovery in patients with complex ulnar neuropathy. Further study to quantify the difference in sensory recovery with traditional operative techniques and cross-cross nerve grafting is required.

PN 105. The Prevalence and Practice Patterns of Human Acellular Nerve Allograft Use in Digital Nerve Gaps: a Survey of Hand Surgeons

Heather Lucas, PA-C¹; Solomon Azouz, MD²; Raman C. Mahabir, MD, MSc¹; Shelley S. Noland, MD
Mayo Clinic, Phoenix, AZ

Introduction:

The use of human acellular nerve allograft (HANA) for digital nerve gaps has become increasingly popular. Current state of adoption and coding practices by hand surgeons has not yet been reported.

Materials & Methods:

A twenty-six-question electronic survey of hand surgeons was performed to evaluate current practice patterns and coding of HANA.

Results:

Of the 461 responses, the majority were trained in orthopedic surgery (76%) or plastic surgery (19%). There was a wide range of years in practice with 38% practicing less than 10 years, 24% practicing 11-20 years, and 36% practicing for more than 20 years. For those who completed a fellowship, 98% completed a hand surgery fellowship, 11% completed a peripheral nerve fellowship, and 7% completed a different fellowship. Most respondents reported using HANA (70%). Of those who do use HANA, nearly all use it less than 10 times/month (98%). There was no significant difference in the use of HANA across different specialties ($p=0.41$) but there was a significant difference in the use of HANA depending on the type of practice ($p=0.0047$), number of years in practice ($p=0.0001$), and the volume of nerve cases per month ($p=0.0367$). For all respondents, when presented with the clinical scenario of a 2 cm digital nerve gap, 39% would use HANA, 35% would use nerve conduit, and 21% would use nerve autograft (Figure 1). The most common CPT code selected was 64910 (nerve repair with synthetic conduit or vein allograft, 49%) followed by 64890 (nerve graft, single strand, hand, <4cm, 27%) (Figure 2).

Conclusions:

The majority of hand surgeons (70%) report using HANA in their practice. For the repair of 2 cm digital nerve gaps, HANA use has surpassed both nerve conduits and nerve autograft. Coding for the use of HANA was inconsistent and there may be a role for further clarification of proper coding.

Figure 1.

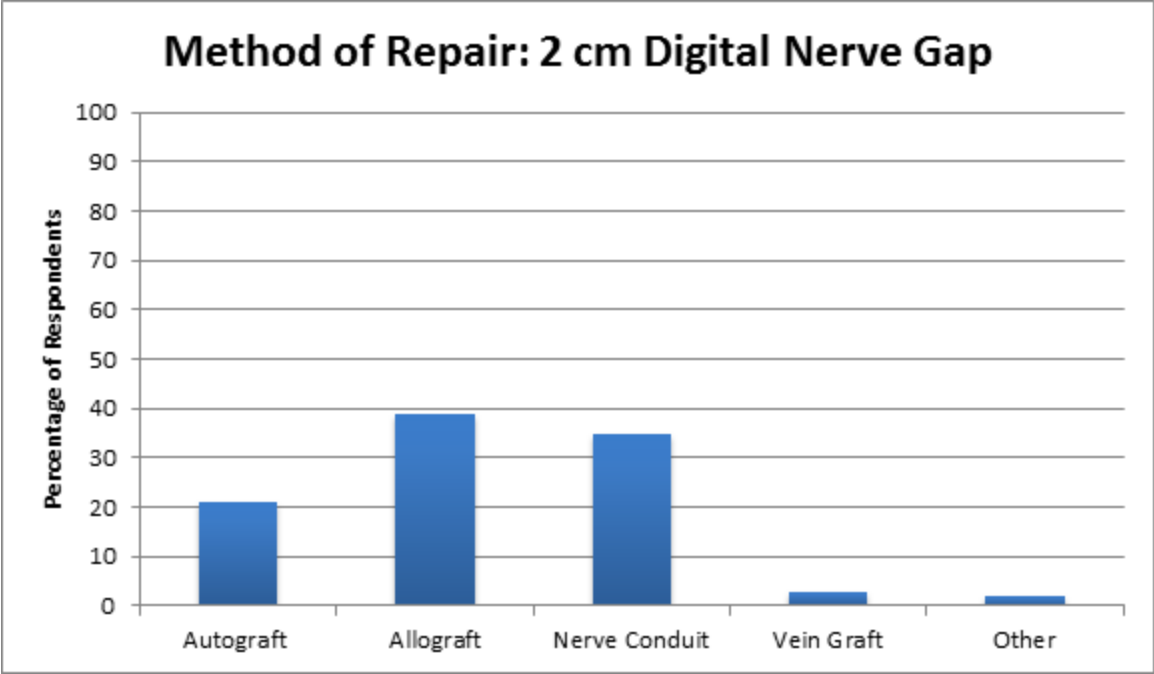


Figure 2.

CPT Code	Nerve Conduit	HANA	Nerve Autograft	Other	Vein Graft
64831	8%	19%	27%	0%	22%
64834	0%	1%	0%	0%	11%
64890	2%	27%	86%	17%	22%
64910	93%	49%	0%	67%	11%
64911	0%	1%	7%	0%	67%
64999	0%	7%	0%	0%	0%

64831: suture of digital nerve, hand or foot, 1 nerve

64834: suture of 1 nerve, hand, common sensory nerve

64890: (nerve graft, single strand, hand, <4cm)

64910: (nerve repair with synthetic conduit or vein allograft)

64911: (nerve repair with autogenous vein graft)

64999: (unlisted procedure nervous system)

PN 106. Quantifying Pain Following Amputation: A Large Scale Outcomes Analysis From 768 Survey Respondents

Lauren M Mioton, MD¹; Jason M. Souza, MD², Mickey S Cho, MD³; Benjamin K Potter, MD²; Scott M Tintle, MD²; Reuben Bueno, MD⁴; George P. Nanos, MD²; Ian Valerio, MD⁵; Jason H Ko, MD¹; Gregory A Dumanian, MD¹

¹Northwestern University, Chicago, IL; ²Walter Reed National Medical Center, Chicago, IL;

³South Texas Orthopedic Specialty Group, San Antonio, TX; (4)Vanderbilt University, Nashville, TN; (5)The Ohio State University, Columbus, OH

Background: Neuroma, stump, and phantom limb pain are all known potential complications following extremity amputation. There are a number of various proposed treatments for any one of the previously listed conditions. However, without a large-scale study providing key baseline data regarding pain following amputation, it is difficult to appropriately measure the impact of treatments on pain in these patients.

Methods: From 2014-2017, patients with a history of upper or lower extremity amputation were invited to take a 80-question online pain survey. Survey data included patient demographics, amputation specific data, as well as stump and phantom pain related questions. Individuals who failed to answer all of the questions were deemed “partial responders” and were excluded from the study.

Results: There were a total of 1203 survey responses; 435 of these were “partial responders” and excluded, leaving 768 surveys for final analysis. Females comprised 33.7% of the respondents. The reason for the amputation was predominantly trauma-related (43.4%), followed by infection (13.2%), cancer (8.1%), ischemia (6.1%), diabetes (5.1%), and congenital defects (4.4%). Most patients had a lower extremity amputation (below the knee amputation, 48.6%; above the knee amputation, 33.6%). A fair number of patients experienced burning “sometimes” or “often” (43.6%) and a quarter of patients reported electrical shocks “often” or “always.” Over two thirds (68.0%) of respondents endorsed phantom limb pain (PLP) and within this group, phantom pain averaged a 5.41 (on a scale of 10) at its worst. A similar number of patients (72.3%) endorsed stump pain, which averaged 5.18 at its worst. Females were more likely to experience stump pain (76.1% vs 70.5%) as well as phantom limb pain (78.0% vs 64.2%). Women also experienced higher average pain scores for both phantom and stump pain. Analysis on the level of amputation shows that an above the elbow amputation led to significantly higher phantom limb and stump pain average scores compared to below the elbow or any lower extremity amputation ($p < 0.05$).

Conclusion: We present the largest study to-date regarding phantom limb, neuroma, and stump pain data in the amputee population. This study provides standard pain measurements for future therapeutic measurements to be compared to. Moreover, we identify high risk subgroups for pain following amputation, including females and those with above the elbow amputations.

PN 107. Osseointegrated Neural Interface (ONI): Evaluating the Capacity to Interface Peripheral Nerves Transposed to Bone Following Amputation for Advanced Prostheses

Aaron M. Dingle, PhD; Joseph R. Novello, MS; Jared P Ness, MS; Jacqueline S. Israel, MD; Lisa Krugner-Higby, DVM, PhD; Brett Nemke, BS; Yan Lu, MD; Weifeng Zeng, MD; Sarah K. Brodnick, BS; Mark D Markel, DVM; Justin C. Williams, PhD; Samuel O. Poore, MD, PhD
University of Wisconsin, Madison, WI

Introduction: Peripheral nerve interfaces represent a paradigm shift in the treatment and prevention of amputation neuromas. Rather than simply bury a transected nerve in muscle or bone in an effort to prevent/treat painful neuromas, attention has moved to exploiting the regenerative capacity of these nerves to power advanced robotic prostheses.

The Osseointegrated Neural Interface (ONI) represents a novel approach to peripheral nerve interfacing; utilizing the medullary cavity of the amputated long bone to house and protect the amputated nerve and the delicate electrode interface. The medullary cavity of long bones is known to be the bone marrow stem cell niche as well as being highly vascular; representing two key components of peripheral nerve tissue engineering and regeneration. This unique environment therefore acts as a native *in vivo* bioreactor for the interfacing severed nerves and electronic prosthetic devices. The purpose of this study was to further develop the ONI model and evaluate the nerve viability in bone at 12 weeks post implantation.

Materials and Methods: Transfemoral amputation was performed in New Zealand white rabbits. Briefly, a transfemoral amputation was performed, and the terminal end of the amputated sciatic was passed through a proximal corticotomy and threaded into the medullary cavity, secured in a PDMS cuff distally. Animals were explored at 5 and 12 weeks via morphological histology and electrophysiology. Electrophysiology was performed terminally, with a penetrating stimulation probe inserted into the distal end of the amputated femur and recording proximally using hook electrodes placed under the nerve external to bone. Monophasic and biphasic pulses of varying amplitudes for 40 μ s duration were recorded at 20kHz with an AM Systems model 2100 stimulator box coupled with a TDT acquisition system.

Results and Discussion: Morphological examination of the amputated sciatic within the bone demonstrated neuroma formation. In animals that received a PDMS cuff, lateral nerve sprouting (S100+ Schwann cells) through the perforations of the PDMS cuff (representing potential electrodes) indicates that three-dimensional sprouting of nerves is possible (n=4). This sprouting was only evident by 12 weeks, and absent at 5 weeks. For animals that did not receive the PDMS cuff (n=4), S100+ Schwann cells take over an increasingly large proportion of the medullary cavity by 12 weeks. Endoneurial collagen deposition increases between 5 and 12 weeks, with small myelinated axons visible. Electrophysiological data at 5 weeks was indistinguishable from noise (n=4); however, action potentials from within the bone are obtainable by 12 weeks (n=4).

PN 108. Poor Patient Understanding of Expectations in Peripheral Nerve Surgery is Ameliorated by Written Surgical Educational Media

Brandon W Smith, MD, MS; Shawn Brown, CMA; Kate Wan-Chu Chang, MA, MS; Lynda Yang, MD, PhD

University of Michigan, Ann Arbor, MI

Introduction: Realistic expectations from peripheral nerve surgery are critical for patient satisfaction. Unrealistic expectations reduce patient satisfaction given the limitations of our procedures. Despite verbal preoperative education, most clinicians can recall instances where the patients expressed unrealistic expectations. We evaluated the impact of a written educational handout on patient expectations after peripheral nerve surgery.

Methods: We recruited patients scheduled to undergo peripheral nerve surgery at a single institution from 2016-2017. During the pre-operative visit, a specialized nurse practitioner reviewed perioperative protocols, risk and benefits of the surgery, and post-operative care. Patients immediately completed a survey to assess their pre-operative understanding of the verbally reviewed information; during the same visit, an additional written handout (containing the reviewed information including expected pain, motor and sensory function recovery) was given to patients in a randomized fashion. At their first post-operative visit, all patients completed the same survey. We applied standard statistical methods to compare (1) the error rate between the with and without written handout groups and (2) the effectiveness of the written handout.

Results: Thirty-nine patients (mean age of 52 years) participated, and 64% were men. Despite immediately preceding verbal instruction, 31% of patients had erroneous (unrealistic) expectations regarding pain. At the post-operative visit, the group that received the written handout reported a 14% more appropriate understanding regarding pain than the group without the handout. For understanding of the expected recovery of motor function, 32% answered incorrectly at the pre-operative visit. Specifically regarding handout effectiveness for pain, in those individual patients who answered the question incorrectly at the pre-operative visit (N=12), 71% of those with the handout (N=5/7) answered correctly at the post-operative visit compared to 40% without the handout (N=2/5). The handout also showed effectiveness in educating patients regarding motor function recovery expectations (38%, 3/8 with versus 25%, 1/4 without the written handout).

Conclusions: Patients undergoing peripheral nerve procedures demonstrate a high baseline level of misunderstanding of postoperative expectations despite standard in-person verbal counseling. This misunderstanding causes significant difficulties for the surgeon to meet surgical expectations, thereby reducing patient satisfaction. We demonstrated that a simple written handout, reiterating surgical expectations, increased patient understanding significantly. Further investigation is needed to evaluate the effect of the handout on patient satisfaction.

PN 301 Dermal Sensory Interfaces to Restore Graded Sensory Feedback from Prostheses

Andrej Nedic, MSE; Daniel Ursu, PhD; Stephen WP Kemp, PhD; Paul S. Cederna, MD; Melanie G. Urbanchek, PhD

University of Michigan, Ann Arbor, MI

INTRODUCTION: To provide optimal functional restoration following limb loss, neuroprostheses will require sensory feedback. Dermal Sensory Interfaces (DSIs) are de-epithelialized skin wrapped around the distal end of transected residual sensory nerves. DSIs transmit electrical pulses to generate afferent sensory nerve action potentials. Our purpose was to characterize reinnervated DSI electrical pulse transduction into afferent compound sensory nerve action potentials (CSNAPs) for restoring graded sensory perception.

MATERIALS & METHODS: Fischer-344 male rats were used. Control groups were: Native Skin (NS, n=5) and Control Nerve (CN, n=5). Experimental groups were: Transected Nerve (TN, n=5) and DSI (n=4). Sural nerves in TN and DSI rats were transected mid-gastrocnemius muscle. For the DSI group, the transected sural nerve was wrapped with a de-epithelialized glabrous skin graft (Fig. 1). Rats recovered for 2 months. Electrical stimulation was then applied on: ankle skin (NS), the sural nerve (CN and TN), or the DSI. CSNAP peak-to-peak voltage (V_{pp}) and percent of stimuli transduced (signal sensitivity) were recorded proximally from the sural nerve.

RESULTS: All DSIs were well revascularized with reinnervation by the sural nerve. Importantly, for DSIs, increasing stimulation amplitude from threshold (T) to T+150 μ A resulted in an anticipated increase in V_{pp} similar to the control NS group (Fig. 2). The slowly rising slope represents the role skin plays in protecting the well-being of nerves and allows for signal modulation when compared with the dramatically steep rise in V_{pp} of CN and TN (p<0.05). There were no significant differences in V_{pp} when varying stimulation frequency for all groups. For DSIs, there was a predictable increase in V_{pp} with pulse width increase (13.5 \pm 7.3 μ V at 30 μ sec to 81.7 \pm 36.0 μ V at 500 μ sec; R²=0.524) with no difference from NS at 100 to 500 μ sec. Most notably DSIs could transduce electrical pulses below 100 μ sec where NS could not. Electrical stimulation applied to DSIs reliably elicited CSNAPs with signal sensitivity \geq 93%.

CONCLUSIONS: DSIs successfully transduced electrical stimulation to CSNAPs that replicate native intact skin. This study suggests that modulating stimulation pulse amplitude or pulse width may provide graded sensory feedback from neuroprosthetic devices in patients with limb loss.

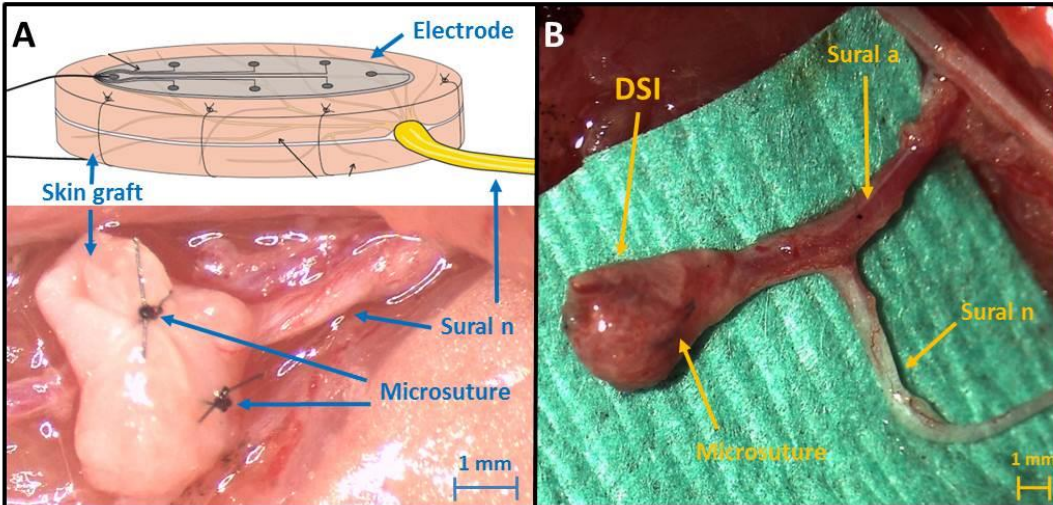


Figure 1. The Dermal Sensory Interface (DSI). (A, TOP) DSI schematic diagram. DSIs consist of residual sensory peripheral nerves implanted into de-epithelialized skin grafts placed subcutaneously. An electrode delivers pulse signaling (from prosthesis force sensors) to the skin graft. (A, BOTTOM) DSI at implantation. The sural n. was transected and placed within a donor de-epithelialized glabrous skin graft. The nerve was in contact with the dermal side of the graft. (B) DSI at 2 months post-implantation. The DSI was healthy with reinnervation from the sural n. Interestingly some DSIs were vascularized by the sural a. Vascularization was not necessary for DSI function.

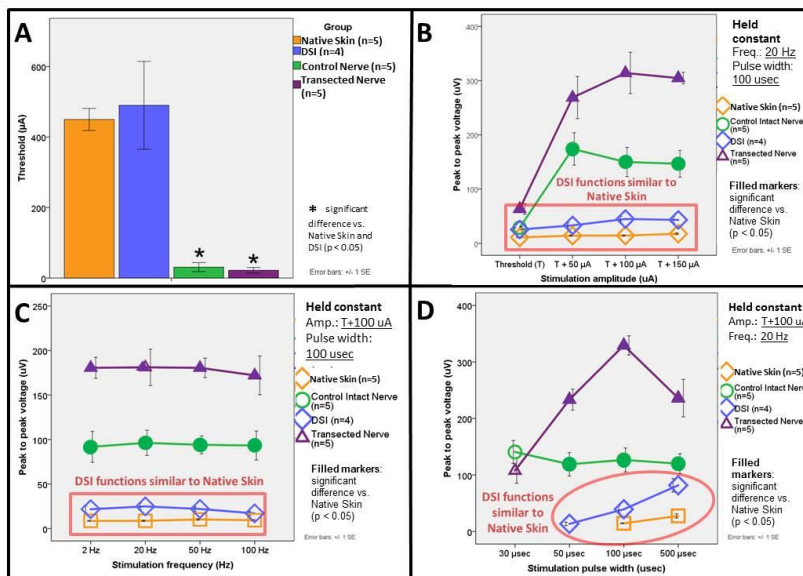


Figure 2. Electrophysiological characterization of DSI function. (A) Minimum current required to elicit CSNAPs (threshold current). DSI and NS had no difference in threshold current. Both groups had significantly higher threshold current compared to CN and TN ($p < 0.05$). The skin acted as a natural resistor protecting nerves from electrical stimulation. (B) CSNAP peak-to-peak voltage (Vpp) response to an increase in electrical stimulation pulse amplitude. There was no difference in DSI and NS function. The slowly rising small increase in Vpp for DSI and NS compared to the dramatic large increase in CN and TN ($p < 0.05$) displays the role skin plays in protecting nerves. (C) CSNAP Vpp response to an increase in electrical stimulation pulse frequency. No differences between DSI and NS function were observed. There was no change in peak-to-peak signaling across 2–100 Hz frequencies for all groups. (D) CSNAP Vpp response to an increase in electrical stimulation pulse width. DSI functioned similarly to NS. The DSI was able to transduce CSNAPs at 50 μsec where NS was not. Without the epithelial skin layer, the DSI was able to transduce pulses across a broader range of pulse widths.

PN 302 Photochemical Tissue Bonding Optimizes Outcomes of Large Gap Peripheral Nerve Defects Repaired with Acellular Nerve Grafts in a Porcine Model

Rachel L Goldstein, DO^{1,2}; Mark A Randolph, MAS1; Gem Runyan, BS, MS¹; Jeena M Easow, MD¹; William S David, MD, PhD; Robert W Redmond, PhD¹; Jonathan M Winograd, MD¹
¹Massachusetts General Hospital, Boston, MA; ²The Wellman Center for Photomedicine, Boston, MA

Background: Standard reconstruction of large gap peripheral nerve defects requires a nerve autograft harvested from a donor limb. This is not always available after massive traumas, as in battlefield situations. An alternative, acellular nerve graft, is associated with suboptimal outcomes. Multiple nerve repair studies demonstrate a benefit using photochemical tissue bonding (PTB) to create a seal of cross-linked collagen across coaptation sites. In our recent small animal studies, PTB improved outcomes when used with acellular grafts to repair large gap nerve defects, compared to standard sutured autograft repair. We now investigate this treatment in a large animal model to achieve clinical relevance.

Materials & Methods: Six miniature swine underwent bilateral ulnar nerve resection. In each pig, 5-cm nerve defects were repaired with sutured saphenous nerve autograft in the control limb, and acellular human nerve graft, Avance®, with PTB in the experimental limb. For PTB, human amniotic membrane (HAM), coated with photosensitizing dye, Rose Bengal, was wrapped around neurorrhaphy sites, then exposed to green light inducing collagen cross-linking. Tacrolimus prevented reaction to xenografts. Functional electromyography (EMG) at the study midpoint and Day 150, measured the compound muscle action potential (CMAP) of the flexor carpi ulnaris (FCU). Graft conduction was measured on Day 150 with direct nerve recording (DNR). On Day 150, animals were euthanized and grafted ulnar nerves and FCU muscles collected for histology.

Results: Five pigs survived the five-month study. There were no gross differences in grafts at harvest. At both the study midpoint and on Day 150, CMAPs in limbs repaired with autologous graft and Avance®/PTB were not statistically different in amplitude (respectively, $p=0.77$ and 0.31) and latency (respectively, $p=0.44$ and 0.75). With DNR, compared to autologous grafts, Avance®/PTB grafts conducted signals with significantly higher amplitude (respectively, 275 ± 138 vs 510 ± 82 μ V, $p=0.03$) and conduction velocity (respectively, 11.7 ± 2.4 vs 28.4 ± 9.7 m/s, $p=0.04$) on Day 150 [FIGURE 1]. On histology, axon regeneration was present distal to both grafts, and FCU muscle fibers appeared similar in both limbs.

Conclusions: When PTB is used with acellular grafts to repair large gap nerve defects, graft conduction is improved and functional electrophysiologic outcomes are comparable to the standard repair. Functionality may be optimized for patients with large gap nerve injuries and no available donor limb by photochemically sealing coaptation sites.

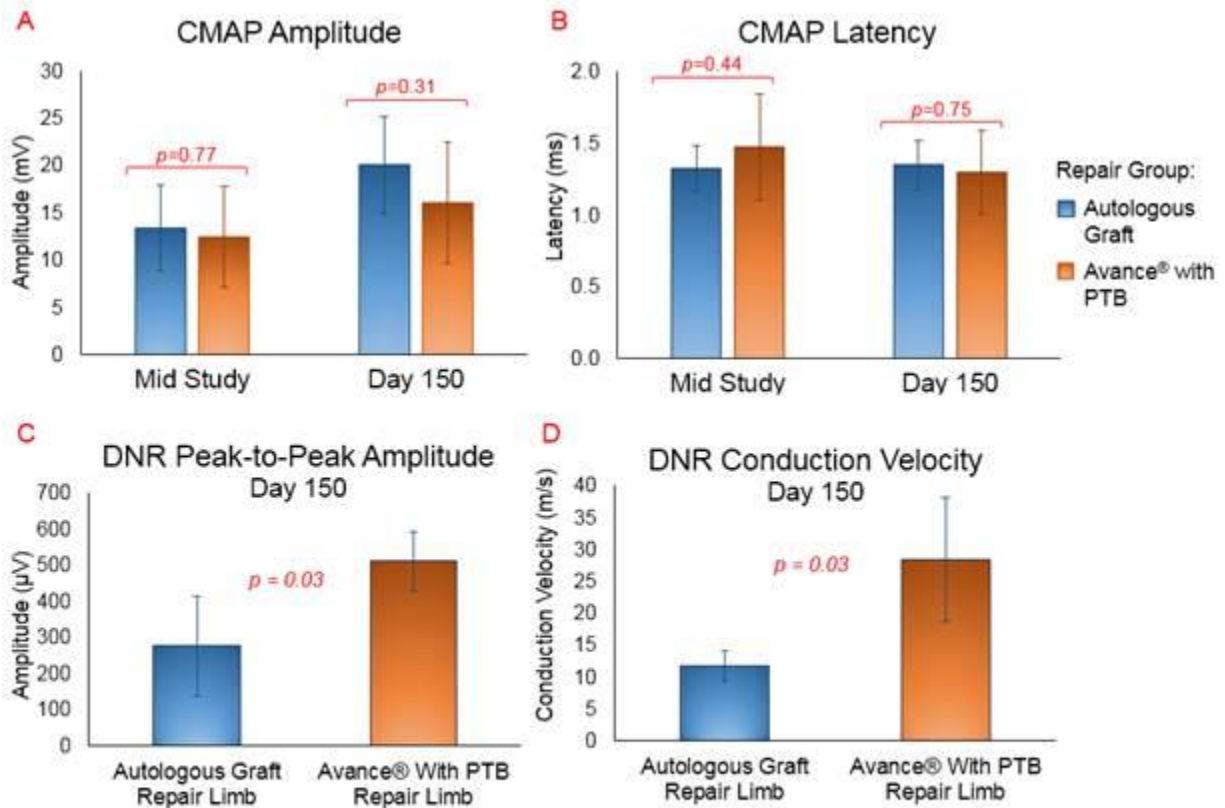


Figure 1: For functional EMG testing, the ulnar nerve was stimulated distal to the graft at the study midpoint and on Day 150 to obtain the CMAP of the FCU (A, B). CMAP amplitude (A) and latency (B) was similar for both groups at both time points. For graft conduction studies using DNR, the ulnar nerve was stimulated proximal and the resulting signal was recorded distal to the graft on Day 150 (C, D). Avance®/PTB grafts conducted signal with significantly higher amplitude (C) and conduction velocity (D) than the autograft.

PN 303 Targeted Muscle Reinnervation in the Leg: An Anatomic Study

Megan Fracol, MD; Lindsay Janes, MD; Jason H Ko, MD; Gregory A. Dumanian, MD
Northwestern University, Chicago, IL

Introduction: Targeted muscle reinnervation (TMR) is a surgical technique to re-route the ends of cut nerves to re-innervate small motor nerves of nearby muscles, with the goal of reducing neuroma pain and/or improving prosthesis function. Anatomical roadmaps for TMR have been established in the upper extremity and thigh, but not for the knee and calf.

Materials and Methods: The major branch points (MBPs) of motor nerves and the motor entry points (MEPs) to muscles of the leg were dissected in five cadaver specimens. Leg length was defined as distance from lateral femoral condyle to lateral malleolus. The distances from the lateral femoral condyle to MBPs and MEPs were measured and these locations were recorded as a percentage of leg length. This information was used to identify targets for TMR in the leg and create a technical roadmap.

Results: The extensor digitorum longus was identified as the best target in the anterior compartment, with an average of 3 MEPs and 1.3 MBs. All cadavers contained a MEP within 50-70% leg length and MB within 20-45% leg length. The peroneus longus was identified as the best target in the lateral compartment, with an average of 5.8 MEPs and 2 MBs. All cadavers contained multiple MEP within 20-40% leg length and a MB within 20-30% leg length. The gastrocnemius was identified as the best target in the superficial posterior compartment, with an average of 4.4 MEPs per muscle head and 1.6 MBs per muscle head. All cadavers contained multiple MEPs within 10-30% leg length and a MB within 0-10% leg length. The flexor digitorum longus was identified as the best target in the deep posterior compartment, with an average of 6 MEPs and 1.7 MBs. All cadavers contained multiple MEPs within 40-70% leg length and a MB within 20-40% leg length. See figure for example of lateral compartment dissection, green arrows demonstrating MEPs to peroneus longus, blue arrows demonstrating MEPs to peroneus brevis, red arrow demonstrating common peroneal nerve bifurcation, yellow arrows demonstrating superficial peroneal nerve sensory branch, white background demonstrating MBs.

Conclusions: TMR is technically feasible in the leg with identifiable superior targets in each compartment. This cadaveric study provides a roadmap for incision placement and identification of motor nerve targets when performing TMR in the leg.

